Check for updates

Received: 25 February 2022 | Revised: 30 April 2022 | Accepted: 4 May 2022

DOI: 10.1002/ardp.202200095

FULL PAPER

ARCH PHARM DPhG
Archiv der Pharmazie

Characterization of caspase-2 inhibitors based on specific sites of caspase-2-mediated proteolysis

Merlin Bresinsky[1] | Jessica M. Strasser[2] | Alexander Hubmann[1] | Bernadette Vallaster[1] | William M. McCue[2] | Jessica Fuller[2] | Gurpreet Singh[2] | Kathryn M. Nelson[2] | Matthew E. Cuellar[2] | Barry C. Finzel[2] | Karen H. Ashe[3,4] | Michael A. Walters[2] | Steffen Pockes[1,2,3]

[1]Institute of Pharmacy, University of Regensburg, Regensburg, Germany

[2]Department of Medicinal Chemistry, University of Minnesota, Minneapolis, Minnesota, USA

[3]Department of Neurology, University of Minnesota, Minneapolis, Minnesota, USA

[4]GRECC, Minneapolis VA Hospital, Minneapolis, Minnesota, USA

Correspondence

Michael A. Walters, Department of Medicinal Chemistry, Institute for Therapeutics Discovery and Development, University of Minnesota, Minneapolis, MN 55414, USA.
Email: mwalters@umn.edu

Steffen Pockes, Institute of Pharmacy, University of Regensburg, Universitätsstraße 31, 93053 Regensburg, Germany.
Email: steffen.pockes@ur.de

Funding information

Lucas Brothers Foundation; Deutsche Forschungsgemeinschaft, Grant/Award Number: Forschungsstipendium 436921318; National Institutes of Health, Grant/Award Number: R01-AG62199; Fonds der Chemischen Industrie, Grant/Award Number: SK-208/16

Abstract

Since the discovery of the caspase-2 (Casp2)-mediated Δtau314 cleavage product and its associated impact on tauopathies such as Alzheimer's disease, the design of selective Casp2 inhibitors has become a focus in medicinal chemistry research. In the search for new lead structures with respect to Casp2 selectivity and drug-likeness, we have taken an approach by looking more closely at the specific sites of Casp2-mediated proteolysis. Using seven selected protein cleavage sequences, we synthesized a peptide series of 53 novel molecules and studied them using in vitro pharmacology, molecular modeling, and crystallography. Regarding Casp2 selectivity, AcITV(Dab)D-CHO (**23**) and AcITV(Dap)D-CHO (**26**) demonstrated the best selectivity (1–6-fold), although these trends were only moderate. However, some analogous tetrapeptides, most notably AcDKVD-CHO (**45**), showed significantly increased Casp3 selectivities (>100-fold). Tetra- and tripeptides display decreased or no Casp2 affinity, supporting the assumption that a motif of five amino acids is required for efficient Casp2 inhibition. Overall, the results provide a reasonable basis for the development of both selective Casp2 and Casp3 inhibitors.

KEYWORDS

Alzheimer's disease, caspase-2, caspase-2 inhibitors, protein cleavage, tauopathies

Abbreviations: AcK, acetylated lysine; AD, Alzheimer's desease; AFC, 7-amino-4- trifluoromethyl coumarin; APS, advanced photon source; AMPA, α-amino-3-hydroxy-5-methyl-4-isoxazolepropionic acid receptor; AU, absorption units; BCA, bicinchoninic acid; Casp1, caspase-1; Casp2, caspase-2; Casp3, caspase-3; Casp4, caspase-4; Casp5, caspase-5; Casp6, caspase-6; Casp7, caspase-7; Casp8, caspase-8; Casp9, caspase-9; Casp10, caspase-10; Casp11, caspase-11; cdock, covalent docking; CHAPS, 3-[(3-cholamidopropyl)dimethylammonio]−1-propanesulfonate; Comp., compound; cpCasp2, circularly permuted caspase-2; D_2O, deuterium oxide; Dab, diaminobutyric acid; Dap, diaminopropionic acid; DIC, *N*,*N*′-diisopropylcarbodiimide; DIPEA, *N*,*N*-diisopropylethylamine; EDCI, 1-ethyl-3-(3-dimethylaminopropyl)carbodiimide; FTD, frontotemporal dementia; HATU, 1-[bis(dimethylamino)methylene]-1H-1,2,3-triazolo[4,5-b]pyridinium 3-oxide hexafluorophosphate; HCl, hydrochloric acid; HD, Huntington's disease; HEPES, 4-(2-hydroxyethyl)−1-piperazineethanesulfonic acid; HOBt, 1-hydroxybenzotriazole hydrate; HRMS, high resolution mass spectrometry; *k*, retention/capacity factor; LBD, Lewy body dementia; MDM2, mouse double minute 2 homolog; MES, 2-(*N*-morpholino)ethanesulfonic acid; MCI, mild cognitive impairment; Orn, ornithine; OXYMA, ethyl cyanohydroxyiminoacetate; PTFE, polytetrafluoroethylene; *R*-Dab, D-isomer of diaminobutyric acid; RFU, relative fluorescence units; *R*-K, D-isomer of lysine; RMSD, root mean square deviation; RO5, Lipinsky's rule of five; RP-HPLC, reversed phase high performance liquid chromatography; SAR, structure affinity relationship; SD, standard deviation; SEM, standard error of the mean; t_0, dead time; SPPS, solid-phase peptide synthesis; UHD, ultrahigh definition.

This is an open access article under the terms of the Creative Commons Attribution License, which permits use, distribution and reproduction in any medium, provided the original work is properly cited.
© 2022 The Authors. *Archiv der Pharmazie* published by Wiley-VCH GmbH on behalf of Deutsche Pharmazeutische Gesellschaft.

1 | INTRODUCTION

In recent years, the caspase-2 (Casp2) enzyme has been increasingly associated with neurodegenerative diseases, specifically tauopathies like Alzheimer's disease (AD), Huntington's disease (HD), frontotemporal dementia (FTD), and Lewy body dementia (LBD).[1–6] Casp2 cleavage of tau at Asp314 generates the cleavage product Δtau314 and leads to synaptic dysfunction and impaired cognition by enabling tau to mislocalize to dendritic spines and reduce AMPA receptors in the postsynaptic membrane.[1,7] The Δtau314 fragment may be a biomarker of impaired cognition, as Δtau314 was increased approximately threefold in brain samples from patients with mild cognitive impairment (MCI) and AD compared to cognitively intact subjects.[1,4] Making tau resistant to Casp2 cleavage preserves memory function and lowering Casp2 restores memory function in mice expressing mutant human tau associated with FTD.[1]

Casp2 is one of the 12 human caspases, a family of cysteine-aspartic proteases, that perform both apoptotic and nonapoptotic effects which include tau cleavage described above.[8–10] In contrast to the other caspase inhibitors, the so far described Casp2 inhibitors have a pentapeptide instead of a tetrapeptide sequence.[11,12] The aspartic acid motif at P1 is also thought to be essential at P4 for binding to the Casp2 enzyme.[13,14] To improve these structures with respect to selectivity and pharmacokinetic properties toward peptidomimetic structures, it is of immense importance to find new peptide sequences that might offer clues to the structural elements that could be used in the design of Casp2 enzyme inhibitors. The cleavage site of tau (GSVQIVYKPVD|LSKVTSKCGSLGNI-; D|L cleavage site), which creates the Δtau314 fragment, and the canonical inhibitor AcVDVAD-CHO were the starting points for the development of recently synthesized Casp2 pentapeptide inhibitors.[15] The appearance of Casp2 within the nucleus, Golgi, and mitochondria enables access to further cellular substrates located in these organelles.[16] Many of these cleavage events can also be mediated by Casp3 or other caspases but some of these peptide sequences have also been reported to be cleaved under physiological conditions only or preferentially by Casp2.[9]

We have selected specific sites of Golgin-160,[17] Protein transport protein sec. 16 A,[18] Transcriptional-regulating factor 1,[18] Ral GTPase-activating protein subunit alpha-1,[18] Holliday junction recognition protein,[18] and MDM2[19] for three reasons: (1) specificity of Casp2 cleavage (except for Holliday junction recognition protein which will serve as a control and SAR point), (2) our interest in characterizing arginine-containing sequences since we have modeling evidence that this basic amino acid will interact with Glu52 in the Casp2 binding site, and (3) noncanonical sequences (sequence ≠ –DXXD–) containing lysine at P2 (Table 1). Our strategy is to start with peptides that represent the cleavage sequences at these sites (Figure 1) and to modify them to exploit specific features in the Casp2 binding pocket, guided by SAR and structural considerations of peptide binding. We expect that the pentapeptides based on these sequences would be an excellent starting point for

TABLE 1 Cleavage sequences of selected substrates specifically and/or efficiently cleaved by caspase-2 (Casp2) and initial synthetic targets.

Protein name, *UniProt designation*	Subsequence/sequence D|X indicates cleavage site	Initial synthetic target	Casp2[a]	k_{cat}/K_m (M^{-1} s^{-1})[b]	Reference
Tau *A0A024RA17 (A0A024RA17_HUMAN)*	YKPV**D|L** GSVQIVYKPV**D|L**SKVTSKCGSLGNI	AcYKPVD-CHO (**1**)	Yes	ND	[1]
Golgin subfamily A member 3 *Q08378 (GOGA3_HUMAN)*	GESP**D|G** NRASTEGESP**D|G**PGQGGLCQNGPTP	AcGESPD-CHO (**3**)	Yes	3.3×10^4	[17]
Protein Transport Protein Sec. 16A *O15027 (SC16A_HUMAN)*	WDRA**D|S** SEAPPGWDRA**D|S**GPTQPPLSLSPAP	AcWDRAD-CHO (**4**)	Yes	5.4×10^3	[18]
Transcriptional-regulating factor 1 *Q96PN7 (TREF1_HUMAN)*	QDTR**D|G** ISPHFPQDTR**D|G**LGLPVGSKNLGQM	AcQDTRD-CHO (**5**)	Yes	1.3×10^3	[18]
Holliday junction recognition protein *Q8NCD3 (HJURP_HUMAN)*	ADRT**D|G** DSSMKPADRT**D|G**SVQAAAWGPELPS	AcADRTD-CHO (**6**)	Casp3 8.3×	1.2×10^3	[18]
E3 ubiquitin-protein ligase Mdm2 P23804 (MDM2_MOUSE)	LDVP**D|G** AQAEEGLDVP**D|G**KKLTENDAKEPCA	AcLDVPD-CHO (**7**)	Yes	ND	[19]
E3 ubiquitin-protein ligase Mdm2 Q00987 (MDM2_HUMAN)	FDVP**D|C** TQAEEGFDVP**D|C**KKTIVNDSRESCV	AcFDVPD-CHO (**8**)	Yes	ND	[19]
Ral GTPase-activating protein subunit alpha-1 *Q6GYQ0 (RGPA1_HUMAN)*	ITVK**D|G** NECLEDITVK**D|G**LSLQFKRFRETVP	AcITVKD-CHO (**9**)	Yes	1.1×10^3	[18]

Abbreviation: ND, not determined.

[a]Is the protein sequence cleaved specifically by Casp2? **6** is cleaved by Casp2 but 8.3× more efficiently by Casp3.

[b]K_{cat}/K_m represents the catalytic efficiency of Casp2.

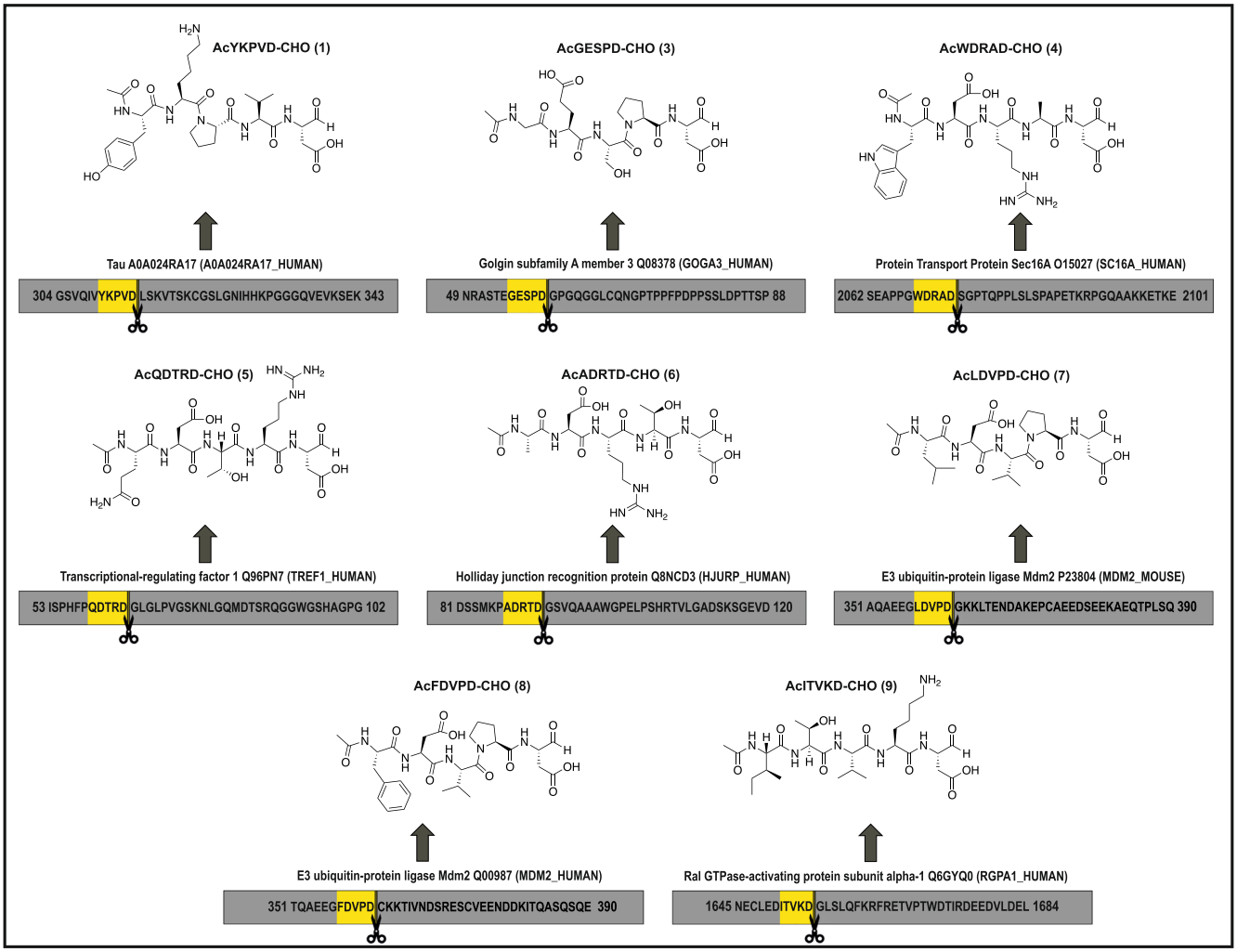

FIGURE 1 Specific caspase-2 cleavage sequences of selected natural proteins and our proposed inhibitors: AcYKPVD-CHO (**1**), AcGESPD-CHO (**3**), AcWDRAD-CHO (**4**), AcQDTRD-CHO (**5**), AcADRTD-CHO (**6**), AcLDVPD-CHO (**7**), AcFDVPD-CHO (**8**), and AcITVKD-CHO (**9**).

probe discovery. New insights into selectivity and drug likeness are needed to effectively develop in vivo Casp2 probes. In this context, novel active peptide sequences could provide important information on where modifications can be made in the molecule, compared to the canonical inhibitors, to achieve the attributes addressed above. Shortening of the pentapeptides to tetra- and tripeptides should give us more information about the importance of the P5/P4 positions and the possibility of decreasing molecular weight for small molecules.

2 | RESULTS AND DISCUSSION

2.1 | Chemistry

Preparation of the aspartic acid-loaded amino-Merrifield resin was carried out according to previously described protocols[20–22] with minor modifications[15] in the sequence of the synthetic steps. The peptides were synthesized by manual solid-phase peptide synthesis (SPPS) on an aspartic acid-loaded amino-Merrifield resin in accordance to the standard Fmoc strategy (see Scheme 1). The Fmoc protection group of the N-terminal amino acid was deprotected with piperidine 20% in DMF (a). The amino acids were coupled to the amino-Merrifield resin by using HATU/DIPEA or Oxyma/DIC (b). The deprotecting and coupling steps were repeated until the desired tri-, tetra-, or pentapeptide was built up. Finally, the N-terminus was acetylated by using acetic anhydride (c). Subsequently, the peptides were cleaved from the resin and the side chains of the amino acids were deprotected by treatment with trifluoroacetic acid (90%) in water (d). Chemical stability of pentapeptides **7**, **38**, **41**, **42**, **43**, **44**, and **55** was analyzed at room temperature for 28 days and is shown in the Supporting Information: Figures S203–S209.

2.2 | Pharmacology

The penta-, tetra-, and tripeptides were investigated in a fluorescence-based enzyme inhibition assay using Casp1, Casp2, Casp3, Casp6, Casp7,

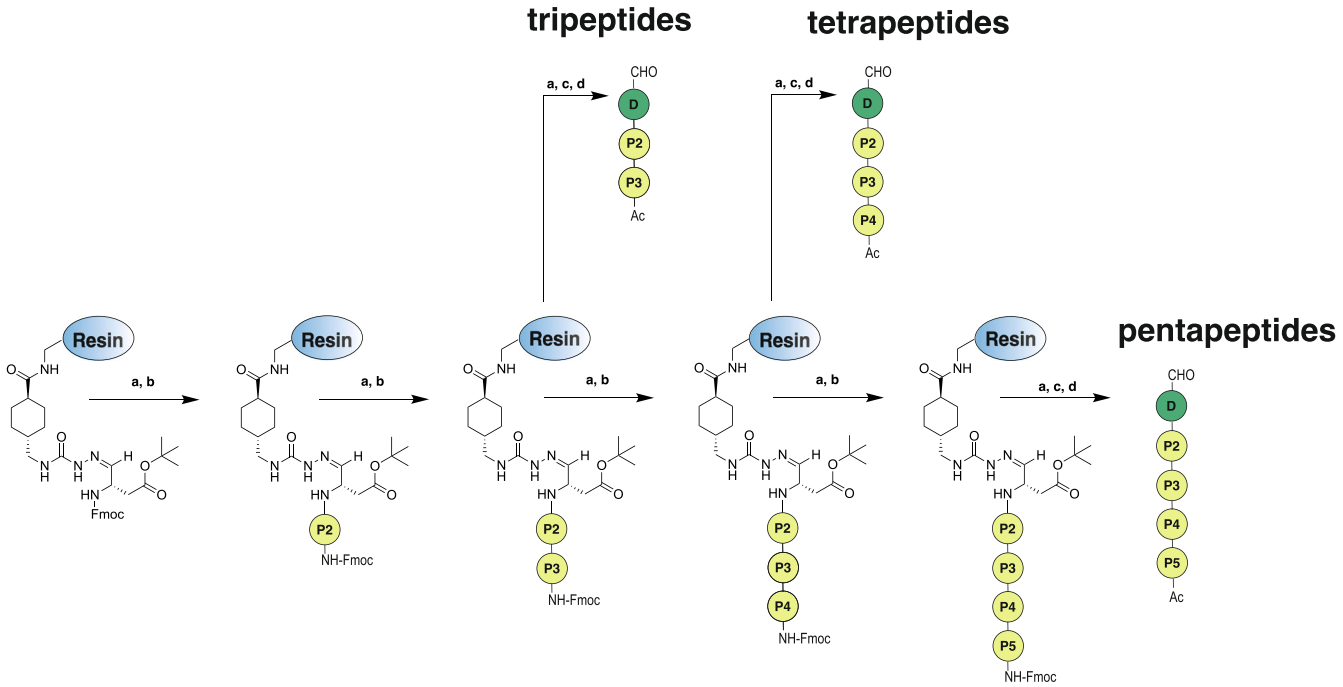

SCHEME 1 Preparation of the peptides on the modified amino-Merrifield resin: (a) piperidine 20% in dimethylformamide (DMF), 35°C, 15 min; (b) amino acid (5 eq), 1-[bis(dimethylamino)methylene]-1*H*-1,2,3-triazolo[4,5-*b*]pyridinium 3-oxide hexafluorophosphate/*N*,*N*-diisopropylethylamine (DIPEA) (5/5 eq) or Oxyma/*N*,*N*′-diisopropylcarbodiimide (5/5 eq), DMF/NMP (8:2 v/v), 35°C, 45 min (single coupling); (c) acetic anhydride (10 eq), DIPEA (10 eq), DMF, rt, 30 min; (d) trifluoroacetic acid (90% in water), rt, 1 h.

and Casp9 to elucidate their structure–affinity relationships and selectivity profile. The results are presented as binding constants (pK_i values) in Table 2 and 3.

The pentapeptide inhibitors based on natural proteins (see Figure 1) cleaved by Casp2 resulted in a series of peptides with distinct affinities. While the inhibitors AcLDVPD-CHO (**7**) and AcFDVPD-CHO (**8**) derived from the MDM2 protein (mouse/human) show high affinities for both Casp2 (pK_i: 7.88/7.66 and 8.15/8.03) and Casp3 (pK_i: 8.16 and 8.52), the inhibitors based on the protein Golgin subfamily A member 3 AcGESPD-CHO (**3**) and Ral GTPase-activating protein subunit alpha-1 AcITVKD-CHO (**9**) demonstrate lower affinities for Casp2 (pK_i: 5.23 and 6.40) and Casp3 (pK_i: 6.73 and 6.05) (Table 2). Interestingly **9** is the first Casp2 inhibitor within our series with the absence of aspartate (Asp) at position 4, showing a moderate affinity for Casp2. The inhibitors AcWDRAD-CHO (**4**) (based on protein transport protein sec. 16A), AcQDTRD-CHO (**5**) (based on Transcriptional-regulating factor 1), and AcADRTD-CHO (**6**) (based on Holliday junction recognition protein) have a moderate inhibitory affinity for Casp2 (pK_i value of 6.73–7.34) with approximately the same affinity for Casp3 (pK_i value of 7.00–7.34) (Table 2). All natural proteins were selected because of their specificity of Casp2 cleavage except for the Holliday junction recognition protein, which serves as a control and SAR point. Apart from this, **3**, **4**, **5**, **6**, **7**, and **8** show a lack of selectivity for Casp2 (selectivity ranging from 0.03 to 1.00), as already seen for **1**[15] (cf. Table 2 and Figure 2). Only AcITVKD-CHO (**9**) exhibits a marginal tendency for Casp2 with a selectivity factor of 2 (cf. Table 2 and Figure 2).

The inhibitors derived from these various natural cleavage sequences (except AcGESPD-CHO (**3**)) were truncated to verify the extent to which this affects the affinities for Casp2 and Casp3. The purpose of shortening was to make the molecules more drug-like with respect to Lipinski's rule of five (RO5)[23] and to pave the way for future small molecules. Truncations of **4** resulted in the tetrapeptide AcDRAD-CHO (**10**) and the tripeptide AcRAD-CHO (**11**). While **10** continues to show affinity for Casp2 (pK_i: 6.39/5.97) and Casp3 (pK_i: 6.59), **11** evidenced a sharp loss in affinity for Casp2 (pK_i: <4) and Casp3 (pK_i: <4). The same can be observed for the tetrapeptides AcDTRD-CHO (**12**), AcDRTD-CHO (**14**), and AcDVPD-CHO (**16**) (Casp2 pK_i: 6.35/6.16, 5.80/5.60, and 6.44/6.33; Casp3 pK_i: 7.09, 7.09, and 8.18) and the respective tripeptides AcTRD-CHO (**13**), AcRTD-CHO (**15**), and AcVPD-CHO (**17**) (Casp2 pK_i: <4; Casp3 pK_i: <4, 4.96, and 5.24) (Table 2). The peptide AcTVKD-CHO (**18**) represents a slightly lower affinity for Casp2 (pK_i: 5.11) and Casp3 (pK_i: 4.95) compared to the other tetrapeptides, which can be explained by the absence of aspartic acid at position 4. In turn, the tripeptide AcVKD-CHO (**19**) completely loses its affinity for Casp2 (pK_i: <4) and Casp3 (pK_i: <4) (Table 2). It can be summarized that the truncation of the pentapeptides by one amino acid is well tolerated for all tetrapeptides (**10**, **12**, **14**, and **16**) containing an aspartic acid at position 4. The loss of affinity for Casp2 and Casp3 is somewhat greater for tetrapeptides having threonine (Thr) at position 4 (e.g., AcTVKD-CHO (**18**)). However, the truncation by a further amino acid is accompanied by a sharp loss in affinity for all tripeptides (**11**, **13**, **15**, **17**, and **19**). Overall, a more significant decrease in Casp2 affinity

TABLE 2 Binding data (pK_i values) and selectivity ratios of peptides **1**–**55** at caspase-2 (Casp2) and caspase-3 (Casp3).

Sequence	Compound	$pK_i \pm SEM$ Casp2	*N*	Casp3	*N*	Selectivity ratios of K_i (Casp2:Casp3)
AcYKPVD-CHO	**1**	4.56 ± 0.43[a,b]	3	4.73 ± 0.10[c]	4	1:1
AcVDVAD-CHO	**2**	7.85 ± 0.08[a]	5	7.73 ± 0.09[c]	5	1:1
AcGESPD-CHO	**3**	5.23 ± 0.12[a]	4	6.73 ± 0.14	3	32:1
AcWDRAD-CHO	**4**	7.34 ± 0.04[a]	2	7.34 ± 0.05	4	1:1
		6.99 ± 0.05[c]	2			2:1
AcQDTRD-CHO	**5**	7.02 ± 0.06[a]	3	7.14 ± 0.16	3	1:1
AcADRTD-CHO	**6**	6.73 ± 0.05[a]	3	7.00 ± 0.09	3	2:1
AcLDVPD-CHO	**7**	7.88 ± 0.01[a]	2	8.16 ± 0.04	4	2:1
		7.66 ± 0.02[b]	2			3:1
AcFDVPD-CHO	**8**	8.15 ± 0.09[a]	2	8.52 ± 0.06	4	2:1
		8.03 ± 0.07[b]	2			3:1
AcITVKD-CHO	**9**	6.40 ± 0.16[a]	4	6.05 ± 0.06	4	1:2
AcDRAD-CHO	**10**	6.39[a]	1	6.67 ± 0.08	3	2:1
		5.99 ± 0.02[b]	2			5:1
AcRAD-CHO	**11**	<4[a]	1	<4	2	-
		<4[b]	2			-
AcDTRD-CHO	**12**	6.35 ± 0.03[a]	2	7.09 ± 0.05	3	5:1
		6.32 ± 0.16[b]	2			5:1
AcTRD-CHO	**13**	<4[a]	2	<4	2	-
AcDRTD-CHO	**14**	5.80 ± 0.02[a]	2	7.09 ± 0.05	3	18:1
		5.49 ± 0.11[b]	2			39:1
AcRTD-CHO	**15**	<4[b]	2	4.96 ± 0.09	2	> 9:1
AcDVPD-CHO	**16**	6.44 ± 0.01[a]	2	8.18 ± 0.12	4	55:1
		6.33 ± 0.03[b]	2			71:1
AcVPD-CHO	**17**	<4[b]	2	5.24 ± 0.04	2	>17:1
AcTVKD-CHO	**18**	5.11 ± 0.04[a]	2	4.95 ± 0.04	2	1:1
AcVKD-CHO	**19**	<4[a]	2	<4	2	-
AcITV(Orn)D-CHO	**20**	6.14 ± 0.12[a]	2	5.68 ± 0.11	2	1:3
		6.14 ± 0.04[b]	2			1:3
AcTV(Orn)D-CHO	**21**	4.62 ± 0.14[a]	2	4.77 ± 0.01	2	1:1
AcV(Orn)D-CHO	**22**	<4[a]	2	<4	2	-
AcITV(Dab)D-CHO	**23**	5.85 ± 0.04[a]	2	5.04 ± 0.11	3	1:6
		5.38 ± 0.18[b]	2			1:2
AcTV(Dab)D-CHO	**24**	4.21 ± 0.11[a]	2	4.43 ± 0.21	2	2:1
AcV(Dab)D-CHO	**25**	4.28 ± 0.18[a]	2	<4	2	>1:2
AcITV(Dap)D-CHO	**26**	5.93 ± 0.58[a]	2	5.32 ± 0.17	3	1:4
		5.48 ± 0.01[b]	2			1:1
AcTV(Dap)D-CHO	**27**	<4[a]	2	4.43 ± 0.21	2	3:1

(Continues)

TABLE 2 (Continued)

Sequence	Compound	pK_i ± SEM Casp2	N	Casp3	N	Selectivity ratios of K_i (Casp2:Casp3)
AcV(Dap)D-CHO	**28**	<4[a]	2	<4	2	-
AcITV(AcK)D-CHO	**29**	6.30 ± 0.06[a]	2	7.34 ± 0.12	3	11:1
		6.24 ± 0.01[b]	2			13:1
AcTV(AcK)D-CHO	**30**	4.70 ± 0.18[a]	2	6.65 ± 0.10	3	89:1
		4.68 ± 0.03[b]	2			93:1
AcV(AcK)D-CHO	**31**	<4[a]	2	5.02 ± 0.15	2	>10:1
AcITGKD-CHO	**32**	5.57 ± 0.01[a]	2	5.75 ± 0.22	2	2:1
AcTGKD-CHO	**33**	4.96 ± 0.03[a]	2	5.47 ± 0.02	2	3:1
AcGKD-CHO	**34**	<4[a]	1	<4	2	-
		<4[b]	2			-
AcITAKD-CHO	**35**	6.63 ± 0.04[a]	3	6.27 ± 0.05	3	1:2
AcTAKD-CHO	**36**	5.79 ± 0.10[a]	2	5.92 ± 0.01	2	1:1
AcAKD-CHO	**37**	<4[a]	1	<4	2	-
		<4[b]	2			-
AcATVKD-CHO	**38**	5.86 ± 0.03[b]	2	5.93 ± 0.05	2	1:1
AcATV(Dab)D-CHO	**39**	4.72 ± 0.02[b]	2	4.68 ± 0.09	2	1:1
AcITVSD-CHO	**40**	6.01 ± 0.10[b]	3	6.24 ± 0.04	3	2:1
AcVDVSD-CHO	**41**	7.26 ± 0.06[b]	3	7.29 ± 0.03	3	1:1
AcDVAD-CHO	**42**	5.95 ± 0.19[b]	3	7.37 ± 0.11	3	26:1
AcVAD-CHO	**43**	<4[b]	2	<4	2	-
AcDVKD-CHO	**44**	6.05 ± 0.07[b]	3	6.61 ± 0.03	3	4:1
AcDKVD-CHO	**45**	5.61 ± 0.06[a]	2	7.79 ± 0.02	4	151:1
		5.22 ± 0.03[b]	2			371:1
AcDV(Dab)D-CHO	**46**	4.93 ± 0.07[b]	2	5.48 ± 0.03	2	4:1
AcITV(*R*-K)D-CHO	**47**	<4[b]	2	<4	2	-
AcITV(*R*-Dab)D-CHO	**48**	<4[b]	2	<4	2	-
AcVDV(*R*-K)D-CHO	**49**	<4[b]	2	<4	2	-
AcVDV(*R*-Dab)D-CHO	**50**	4.41 ± 0.05[b]	2	<4	2	>1:3
AcVD(*R*-K)VD-CHO	**51**	<4[b]	3	6.04 ± 0.02	3	>110:1
AcVD(*R*-Dab)VD-CHO	**52**	4.19 ± 0.14[b]	2	5.64 ± 0.06	2	28:1
AcVD(*R*-K)AD-CHO	**53**	4.31 ± 0.26[b]	2	<4	2	>1:2
AcVD(*R*-Dab)AD-CHO	**54**	<4[b]	2	0.71 ± 0.06	2	>5:1
AcTDTAD-CHO	**55**	7.48 ± 0.14[a]	2	7.22 ± 0.12	3	1:2
		7.19 ± 0.15[b]	2			1:1

Note: Data shown are mean values ± SEM of *N* independent experiments, each performed in duplicate or triplicate. Data were analyzed by nonlinear regression and were best fitted to sigmoidal concentration–response curves. Conversion of this table data to K_i values within the 95% confidence interval is shown in Supporting Information: Table S2.

[a]Data represent pK_i values determined with Casp2.

[b]Data (pKi ± SD) described in Bresinsky et al.[15]

[c]Data represent pK_i values determined with cpCasp2.

TABLE 3 Binding data (pK_i values) of selected peptides (**1**–**9**, **16**, **26**, **29**, **35**, and **45**) at caspase (Casp)1, Casp6, Casp7, and Casp9.

		pK_i ± SEM							
Sequence	Compound	Casp1	*N*	Casp6	*N*	Casp7	*N*	Casp9	*N*
AcYKPVD-CHO	**1**	<4[a]	2	<4[a]	2	4.53 ± 0.19[a]	2	<4.5[a]	2
AcVDVAD-CHO	**2**	7.06 ± 0.06[a]	2	<4[a]	2	7.08 ± 0.06[a]	2	5.57 ± 0.31[a]	2
AcGESPD-CHO	**3**	6.52 ± 0.10	2	<4	2	5.72 ± 0.01	2	5.61 ± 0.11	2
AcWDRAD-CHO	**4**	6.48 ± 0.02	2	4.64 ± 0.03	2	6.83 ± 0.01	2	4.96 ± 0.05	2
AcQDTRD-CHO	**5**	5.5 ± 0.01	2	<4	2	6.55 ± 0.03	2	<4	2
AcADRTD-CHO	**6**	5.83 ± 0.07	2	<4	2	6.93 ± 0.07	2	4.81 ± 0.14	2
AcLDVPD-CHO	**7**	7.30 ± 0.02	2	4.57 ± 0.08	2	7.68 ± 0.01	2	5.66 ± 0.10	2
AcFDVPD-CHO	**8**	7.34 ± 0.07	2	4.85 ± 0.04	2	8.07 ± 0.11	2	5.98 ± 0.57	2
AcITVKD-CHO	**9**	6.35 ± 0.06	2	5.48 ± 0.07	2	5.25 ± 0.14	2	4.46 ± 0.35	2
AcDVPD-CHO	**16**	7.15 ± 0.05	2	<4	2	7.74 ± 0.07	2	6.32 ± 0.08	2
AcITV(Dap)D-CHO	**26**	5.82 ± 0.29	2	4.42 ± 0.37	2	4.61 ± 0.47	2	4.68 ± 0.02	2
AcITV(AcK)D-CHO	**29**	6.74 ± 0.19	2	6.01 ± 0.39	2	6.65 ± 0.05	2	5.33 ± 0.04	2
AcITAKD-CHO	**35**	5.84 ± 0.04	2	4.69 ± 0.02	2	5.48 ± 0.02	2	4.59 ± 0.12	2
AcDKVD-CHO	**45**	6.17 ± 0.06	2	<4	2	7.51 ± 0.10	2	5.41 ± 0.05	2

Note: Data shown are mean values ± SEM of *N* independent experiments, each performed in duplicate or triplicate. Data were analyzed by nonlinear regression and were best fitted to sigmoidal concentration–response curves.

[a]Data (pK_i ± SD) described in Bresinsky et al.[15]

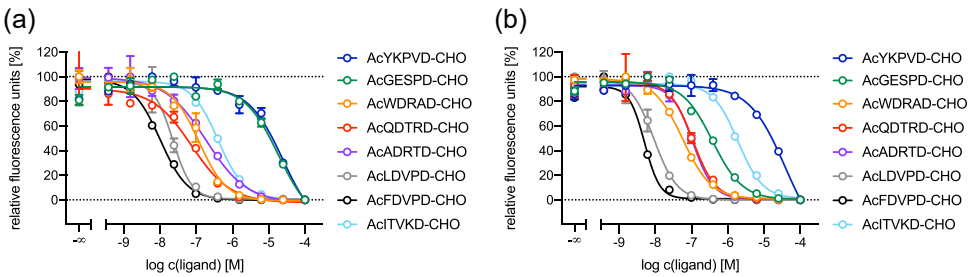

FIGURE 2 Concentration-response curves of AcYKPVD-CHO (**1**), AcGESPD-CHO (**3**), AcWDRAD-CHO (**4**), AcQDTRD-CHO (**5**), AcADRTD-CHO (**6**), AcLDVPD-CHO (**7**), AcFDVPD-CHO (**8**), and AcITVKD-CHO (**9**) at caspase-2 (a) and caspase-3 (b) in the fluorimetric enzyme assay. Data points represent mean values ± SD from representative experiments, each performed in duplicate.

(ranging from 0.67 to 1.70 logarithmic units) than Casp3 (ranging from 0.20 to 0.75 logarithmic units) can be observed for all tetrapeptides. In case of AcDRTD-CHO (**14**) and AcDVPD-CHO (**16**) even a slight increase (ranging from 0.02 to 0.09 logarithmic units) in Casp3 affinity can be observed compared to AcADRTD-CHO (**6**) and AcLDVPD-CHO (**7**) (Table 2). These observations go hand-in-hand with the assumption that a motif of five amino acids is required for efficient Casp2 inhibition. Regarding the tetrapeptide's selectivity between Casp2 and Casp3, it can be observed that **10**, **12**, **14**, and **16** are showing a trend toward Casp3 selectivity (2–71-fold), whereas **18** demonstrates no trend in selectivity (Table 2).

Due to the fact that AcITVKD-CHO (**9**) shows the best Casp2 selectivity profile, further inhibitors based on **9** were developed to gain more insight into the structure–affinity relationships between our peptides and the Casp2/Casp3 binding site. Moreover, **9** is the only reasonably active Casp2 inhibitor that we prepared that does not contain an aspartic acid at the P4 position, which should be beneficial for its pharmacokinetic properties. The Casp2 inhibitor AcVDV(Dab)D-CHO,[15] just recently synthesized in our laboratory, served as a starting point for this series. This peptide inhibitor has affinities of pK_i: 7.26 (Casp2) and pK_i: 5.82 (Casp3), displaying a 27.7-fold Casp2 selectivity over Casp3.[15] The stepwise shortening of the side chain and the acetylation of lysine at P2 led to the peptides AcITV(Orn)D-CHO (**20**; Casp2 pK_i: 6.14; Casp3 pK_i: 5.68), AcITV(Dab)D-CHO (**23**; Casp2 pK_i: 5.85/5.56; Casp3 pK_i: 5.04), AcITV(Dap)D-CHO (**26**; Casp2 pK_i: 5.93/5.48; Casp3 pK_i: 5.32), and AcITV(AcK)D-CHO (**29**; Casp2 pK_i: 6.30/6.23; Casp3 pK_i: 7.34), all of them showing lower affinities for Casp2 (Table 2). While **20**, **23**, and **26** demonstrate

lower affinities for Casp3, AcITV(AcK)D-CHO (**29**) has a higher affinity for Casp3 than **9**. In terms of selectivity, we found a selectivity advantage for Casp2 over Casp3 due to the stepwise shortening of the lysine sidechain. While **9** (containing lysine) has a selectivity factor of 2, **20** (containing ornithine) exhibits a factor of 3, **23** (containing diaminobutyric acid) of 6 or 3, respectively, and **26** (containing diaminopropionic acid) of 4 or 1, respectively (Table 2). The acetylation of lysine (AcITV(AcK)D-CHO, **29**) generates a selectivity shift toward Casp3 (Casp3/Casp2 selectivity 11 or 13, respectively). The inhibitors **20**, **23**, **26**, and **30** were also truncated to get a deeper insight into the structure–affinity relationship of tetra- and tripeptides and the target enzymes. This resulted in the tetrapeptides AcTV(Orn)D-CHO (**21**; Casp2 pK_i: 4.62; Casp3 pK_i: 4.77), AcTV(Dab)D-CHO (**24**; Casp2 pK_i: 4.21; Casp3 pK_i: 4.43), and AcTV(Dap)D-CHO (**27**; Casp2 pK_i: <4; Casp3 pK_i: 4.43) which show slightly lower affinities for Casp2 and Casp3 relative to AcTVKD-CHO (**18**) (Table 2). While AcTV(AcK)D-CHO (**30**, Casp2 pK_i: 4.70; Casp3 pK_i: 6.65) represents low affinity for Casp2, the affinity for Casp3 almost remains. Thus, the peptide displays selectivity for Casp3 over Casp2 (Casp3/(cp)Casp2 selectivity 89 or 93) (Table 2). The corresponding tripeptides of this series AcV(Orn)D-CHO (**22**), AcV(Dab)D-CHO (**25**), AcV(Dap)D-CHO (**28**), and AcV(AcK)D-CHO (**31**) do not show notable affinity for Casp2 (pK_i values < 4) nor Casp3 (pK_i values < 4 to 5.02) (Table 2).

Starting from AcITVKD-CHO (**9**) further modifications were made, for example, valine at position P3 was replaced by glycine and alanine. At the same time, we prepared tetra- and tripeptides of these sequences. This resulted in AcITGKD-CHO (**32**), AcTGKD-CHO (**33**), AcGKD-CHO (**34**), AcITAKD-CHO (**35**), AcTAKD-CHO (**36**), and AcAKD-CHO (**37**). The pentapeptide **32** (Casp2 pK_i: 5.57; Casp3 pK_i: 5.75) shows slightly lower affinity for Casp2 and Casp3 than **9** (Casp2 pK_i: 6.40; Casp3 pK_i: 6.05), whereas the affinities maintained for **35** (Casp2 pK_i: 6.63; Casp3 pK_i: 6.27). Tetrapeptides **33** (Casp2 pK_i: 4.96; Casp3 pK_i: 5.47) and **36** (Casp2 pK_i: 5.79; Casp3 pK_i: 5.92) show lower affinities for Casp2 and Casp3 than the corresponding pentapeptides (Table 2) but the affinity decrease is more pronounced for Casp2 (0.61 and 0.84) than for Casp3 (0.28 and 0.37). The tripeptides **34** and **37** did not show any affinity for Casp2 (pK_i: <4) and Casp3 (pK_i: <4). We have also replaced isoleucine at position P5 by alanine resulting in AcATVKD-CHO (**38**, Casp2 pK_i: 5.86; Casp3 pK_i: 5.93). AcATV(Dab)D-CHO (**39**, Casp2 pK_i: 4.72; Casp3 pK_i: 4.68) was an unsuccessful approach to gain selectivity for Casp2 by exchanging lysine at P2 with diaminobutyric acid (Dab). In addition, we have introduced serine at position P2, but the expected selectivity advantage for Casp2 described by Poreba et al.[24] could not be determined for AcITVSD-CHO (**40**, Casp2 pK_i: 6.01; Casp3 pK_i: 6.24) (Table 2).

To establish further structure–affinity relationships with respect to our recent study by Bresinsky et al.,[15] we made further modifications starting from the already described canonical inhibitor AcVDVAD-CHO (**2**, Casp2 pK_i: 7.85; Casp3 pK_i: 7.73). First, we truncated the pentapeptide to a tetra- and tripeptide, resulting in AcDVAD-CHO (**42**) and AcVAD-CHO (**43**). **42** demonstrates a massive loss of affinity for Casp2 (pK_i: 5.95) by two logarithmic units, while the affinity for Casp3 (pK_i: 7.37) is almost completely preserved (Table 2). Thus, AcDVAD-CHO (**42**) shows a selectivity factor of 26 for Casp3 over Casp2. The tripeptide **43** completely loses its inhibitory affinity for Casp2 (pK_i: <4) and Casp3 (pK_i: <4). We also introduced serine at position P2 of the canonical inhibitor in an attempt to gain selectivity for Casp2 but again the desired effect could not be detected for AcVDVSD-CHO (**41**, Casp2 pK_i: 7.26; Casp3 pK_i: 7.29) (Table 2). AcDVKD-CHO (**44**), AcDKVD-CHO (**45**), and AcDV(Dab)D-CHO (**46**) are the corresponding tetrapeptides of the peptides AcVDVKD-CHO (Casp2 pK_i: 7.63; Casp3 pK_i: 6.91), AcVDKVD-CHO (Casp2 pK_i: 7.40; Casp3 pK_i: 7.28), and AcVDV(Dab)D-CHO (Casp2 pK_i: 7.26; Casp3 pK_i: 5.82) which we have recently described.[15] While for AcDVKD-CHO (**44**) and AcDKVD-CHO (**45**) a significant decrease in affinity for Casp2 (pK_i: 5.99 and 5.61/5.22) can be observed, the affinity for Casp3 (pK_i: 6.62 and 7.79) remains. In the case of **45**, the affinity for Casp3 even increases, making the tetrapeptide a selective Casp3 inhibitor with a selectivity factor of 151 or 371, respectively. AcDV(Dab)D-CHO (**46**) shows low affinity for Casp2 (pK_i: 4.93) and Casp3 (pK_i: 5.48) (Table 2).

Finally, AcITV(*R*-K)D-CHO (**47**), AcITV(*R*-Dab)D-CHO (**48**), AcVDV(*R*-K)D-CHO (**49**), AcVDV(*R*-Dab)D-CHO (**50**), AcVD(*R*-K)VD-CHO (**51**), AcVD(*R*-Dab)VD-CHO (**52**), AcVD(*R*-K)AD-CHO (**53**), and AcVD(*R*-Dab)AD-CHO (**54**) were synthesized to potentially better address specific amino acids (Glu52) in the Casp2 binding site due to the changed spatial arrangement of the inhibitors. Compounds **47**, **48**, **49**, **50**, **53**, and **54** demonstrate low affinities for Casp2 (pK_i values < 4–4.41) and Casp3 (pK_i values < 4–4.71). **51** and **52** show low affinities for Casp2 (pK_i values < 4–4.19) and moderate affinities for Casp3 (pK_i values 6.04 and 5.64). AcVD(*R*-K)VD-CHO (**51**) indicates an at least 100-fold selectivity for Casp3 compared to Casp2 (Table 2). AcTDTAD-CHO (**55**) represents a precursor for future stapled peptides. It displays high affinities for Casp2 (pK_i: 7.48/7.04) and Casp3 (pK_i: 7.22) with no distinct selectivity trend (Table 2).

In addition, a panel assay at Casp1, Casp6, Casp7, and Casp9 (Table 3) was carried out for selected peptides (**3–9**, **16**, **26**, **29**, **35**, and **45**). The pentapeptides AcGESPD-CHO (**3**) and AcADRTD-CHO (**6**) show moderate inhibitory affinities for Casp1 (pK_i: 6.52 and 5.83), Casp7 (pK_i: 5.72 and 6.93), and Casp9 (pK_i: 5.61 and 4.81) and no affinity for Casp6 (pK_i: <4). AcWDRAD-CHO (**4**) and AcQDTRD-CHO (**5**) exhibit moderate affinities for Casp1 (pK_i: 6.48 and 5.51) and Casp7 (pK_i: 6.83 and 6.55) and low affinities for Casp6 (pK_i: 4.64 and <4) and Casp9 (pK_i: 4.96 and <4) (Table 3). AcLDVPD-CHO (**7**, Casp1 pK_i: 7.30; Casp6 pK_i: 4.57; Casp7 pK_i: 7.68; Casp9 pK_i: 5.66) and AcFDVPD-CHO (**8**, Casp1 pK_i: 7.34; Casp6 pK_i: 4.85; Casp7 pK_i: 8.07; Casp9 pK_i: 5.98) derived from the MDM2 protein (mouse/human) are highly active for Casp1 and Casp7. The affinity for Casp9 is lower, while for Casp6 no noticeable affinity can be observed (Table 3). The peptide AcITVKD-CHO (**9**) exhibits moderate to low affinity for Casp1 (pK_i: 6.35), Casp6 (pK_i: 5.48), Casp7 (pK_i: 5.25), and Casp9 (pK_i: 4.46). In comparison, the peptide AcYKPVD-CHO (**1**) shows no major affinity for Casp1, Casp6, Casp7, and Casp9, while the canonical inhibitor AcVDVAD-CHO (**2**) is active at Casp1 (pK_i: 7.06), Casp7 (pK_i: 7.08), and Casp9 (pK_i: 5.57) (Table 3). The tetrapeptide AcDVPD-CHO (**16**, Casp1 pK_i: 7.15; Casp6 pK_i: < 4; Casp7 pK_i: 7.74; Casp9 pK_i:

6.32) shows a similar affinity profile as AcLDVPD-CHO (**7**) and AcFDVPD-CHO (**8**) (Table 3). AcITV(Dap)D-CHO (**26**) indicates slightly lower affinities for Casp1, Casp6, Casp7, and Casp9 compared to lead compound AcITVKD-CHO (**9**) (Casp1 p*K*i: 6.35 vs. 5.82; Casp6 pK_i: 5.48 vs. 4.42; Casp7 pK_i: 5.25 vs. 4.61; Casp9 pK_i: 4.46 vs. 4.68), while AcITV(AcK)D-CHO (**29**) exhibits slightly higher affinities (Casp1 p*K*i: 6.74; Casp6 pK_i: 6.01; Casp7 pK_i: 6.65; Casp9 pK_i: 5.33). Finally, AcITAKD-CHO (**35**) demonstrates moderate to low affinities for Casp1 (pK_i: 5.84), Casp6 (pK_i: 4.69), Casp7 (pK_i: 5.48), and Casp9 (pK_i: 4.59) (Table 3) and AcDKVD-CHO (**45**) displays high affinity for Casp7 (pK_i: 7.51), moderate affinity for Casp1 (pK_i: 6.17), Casp9 (pK_i: 5.41), and low affinity for Casp6 (pK_i: <4) (Table 3).

2.3 | Molecular modeling

To test whether the relative binding affinities of these inhibitors could be understood computationally we implemented a covalent inhibitor docking protocol employing the CovDock module of the Schrödinger Software Suite (Schrödinger, LLC, Version 2021.3 unless otherwise noted).[25–33] We recently reported that ligand poses predicted by this method recapitulate crystallographically determined structures of similar pentapepties with good fidelity.[15] Table 4 lists the covdock affinity results from this protocol for three reference compounds and the new inhibitors reported in this study. The docking results give a good indication of good and bad binders to Casp2 and Casp3, although they do not entirely match the in vitro results from Table 2. However, the consistency of the poor pK_i and cdock affinity values for AcYKPVD-CHO (**1**) (Casp2 and Casp3), as well as the increased cdock affinities for AcQDTRD-CHO (**5**), AcITVKD-CHO (**9**) and AcITV(Dap)D-CHO (**26**) at Casp2 is noticeable. For compounds **9** and **26**, preferential binding to Casp2 over Casp3 is observed both in vitro and in silico.

Additionally, we wondered whether the initial structure of the ligand, since this is generated by methods that are not easily standardized, would affect the final cdock affinity. Cdock affinities were computed starting from five conformations of AcVDVAD-CHO with relative energies spanning 10 kcal/mol (Figure 3). This experiment confirmed that cdock affinities are dependent on the starting conformation of the ligand (at least for these highly flexible ligands) and vary in this simple case over a range of 1.0 kcal/mol with an average value of −13.92 kcal/mol (SD 0.41 kcal/mol, Supporting Information: Table S3). For potent ligands like AcVDVAD-CHO, the final five structures that were arrived at by cdock optimization were roughly identical (root mean square deviation [RMSD] = 0.103–0.067, Supporting Information: Table S4) whereas for weak ligands, like AcYKPVD-CHO, the final structures were significantly different (RMSD = 0.153–0.977, Supporting Information: Table S4).

From these experiments, we conclude that cdock optimization for this class of pentapeptide inhibitors is useful for generally determining whether or not a ligand will bind to the target. If the pentapeptide inhibitor has a cdock affinity <−11.0 kcal/mol, the predicted structure from any starting point will be a good approximation of the crystal structure. Further results along these lines will be reported in due course.

TABLE 4 Molecular modeling of caspase-2 (Casp2) and caspase-3 (Casp3) and potential ligands.

Sequence	Compound	Casp2 cdock affinity	Casp3 cdock affinity
AcYKPVD-CHO	**1**	−9.561	−10.126
AcGESPD-CHO	**3**	−13.073	−12.564
AcWDRAD-CHO	**4**	−13.771	−12.706
AcQDTRD-CHO	**5**	−15.376	−13.369
AcADRTD-CHO	**6**	−13.113	−12.475
AcLDVPD-CHO	**7**	−13.080	−13.271
AcFDVPD-CHO	**8**	−12.728	−13.634
AcITVKD-CHO	**9**	−15.328	−13.100
AcDVPD-CHO	**16**	−11.856	−11.896
AcITV(Dab)D-CHO	**23**	−12.972	−12.876
AcITV(Dap)D-CHO	**26**	−14.278	−12.721
AcDKVD-CHO	**45**	−12.641	−11.952
Reference compounds			
AcVDVAD-CHO	**2**	−13.614	−12.148
AcLDESD-CHO	**56**	−13.519	−13.369
AcDEVD-CHO	**57**	−13.439	−12.218

Note: Calculation using covalent docking in Schrödinger 2021.3. Casp2 = PDBid: 1pyo, Casp3 = PDBid: 3edq. Proteins and ligands prepared as described in the Section 4.2. cdock affinity = covalent docking affinity (kcal/mol).

2.4 | Crystallography

While there has been some exploration of the structural consequences of variation of the P4 amino acid from the preferred aspartic acid in complexes with Casp3[34] and Casp7,[35,36] these have been limited to tetrapeptide inhibitors, and none have specifically involved the P4 threonine found to be preferred from our work. Motivated by curiosity regarding details of how the threonine substitutes for the well-characterized aspartic acid, crystallographic studies were initiated and complexes of five inhibitors with caspase 3 were obtained: one with compound **9** (AcITVKD-CHO), with **16** (AcDVPD-CHO), with **20** (AcITV(Orn)D-CHO), with compound **23** (AcITV(Dab)D-CHO), and one with **36** (AcITAKD-CHO). A summary of crystallographic data and refinement statistics is provided in Supporting Information: Table S1. In the 1.9 Å complex with **23** (AcITV(Dab)D-CHO), the position of the N-terminal acetyl group is not resolved, but in other structures, the ligand backbone geometry is otherwise well-defined by electron density across the length of the pentapeptide. As expected, the CHO leaving group has been displaced and a covalent bond joins the P1 Asp to Cys163, in both structures. The P4 Thr

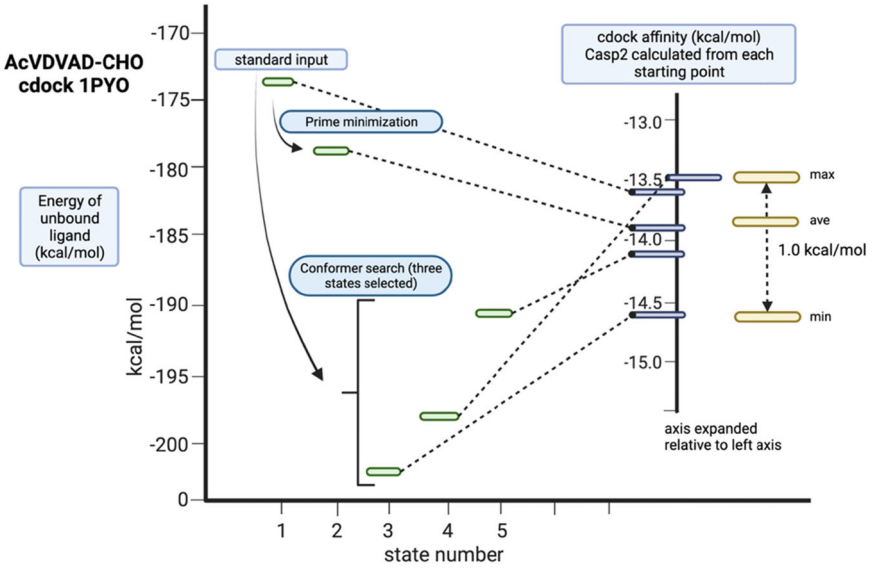

FIGURE 3 The cdock affinities (right axis (kcal/mol)) resulting from the docking of five different conformations of AcVDVAD-CHO (energies on left axis (kcal/mol)) with PDBid: 1 pyo. Energies on the left axis calculated with prime using the OPLS4 forcefield. Energies on the right axis calculated using Glide and the Covalent Docking module in Maestro (Schrödinger, 2021.3).

sidechain occupies the same position and engages in similar H-bonding in these two structures.

A comparison of the complex of compound **23** to a more typical canonical inhibitor sequence (the AcVDVAD-CHO complex previously described by Bresinsky et al.[15]) is provided in Supporting Information: Figure S1. Backbone H-bonds observed in the two complexes are the same, but the lone hydroxyl group of the threonine sidechain (T_4) is not capable of accepting hydrogen bonds from both Phe250 and Asn208 as can a D_4 carboxylate. Only the hydrogen bond from the T_4 OH to Phe250 NH is observed. We had imagined that this might cause either the inhibitor to slide away from L4 toward Asn208 and L3, or L4 to move in tighten packing against the inhibitor with a smaller footprint, but neither change has occurred. The threonine seems to be an isosteric substitute for aspartic acid in P4, albeit with a predictable loss in potency due to the loss of one H-bond.

A comparison of the complexes with compounds **16** and **23** is also provided as in Supporting Information: Figure S1. Backbone H-bonds are conserved in both complexes, illustrating that truncation of pentapeptides to tetrapeptides does not affect the backbone binding conformation. Interestingly, a proline in the tetrapeptide sequence does not alter the backbone binding confirmation either (Supporting Information: Figure S1), leading to the hypothesis that the ring in the proline structure locks the peptide into the binding confirmation. Limiting the number of possible binding confirmations creates a more favorable enthalpy of binding (Gibbs free energy of binding) and could help explain the increase in potency of compound **16** at both Casp2 and Casp3 as compared to other tetrapeptides in the series (e.g., compound **42** [AcDVAD-CHO] and compound **44** [AcDVKD-CHO]).

3 | CONCLUSION

In this study, we report the design and characterization of peptidic caspase-2 inhibitors originating from specific sites of Casp2-mediated proteolysis. Besides the classic key motif of Casp2 inhibitors, consisting of five amino acids, we have also truncated our inhibitors to tetrapeptides and tripeptides which should result in a better bioavailability and a more drug-like character of our ligands relative to Lipinski's RO5. In summary, we have synthesized and characterized a series of 53 peptides for their inhibitory affinity at Casp2 and Casp3. Selected inhibitors **3**–**9**, **16**, **23**, **26**, **29**, **35**, and **45** were tested in a panel assay screening to examine affinities at Casp1, Casp6, Casp7, and Casp9 to receive more information about the selectivity within the caspase family. Within the new cleavage sequences, the inhibitors AcLDVPD-CHO (**7**) and AcFDVPD-CHO (**8**) demonstrate the highest affinity for Casp2 (pK_i: 7.88/7.66 and 8.15/8.03). Nevertheless, it must be noted that **7** and **8** display little selectivity for Casp2 over Casp3 (Casp2/Casp3 selectivity: 2–3). Truncation of **7** and **8** resulted in the tetrapeptide AcDVPD-CHO (**16**, Casp2 pK_i: 6.44/6.33; Casp3 pK_i: 8.18) with **16** showing Casp3 selectivity. Overall the truncation of pentapeptides to tetra- and tripeptides does not lead to Casp2 selectivity. In the case of tripeptides, even a total collapse of Casp2 and Casp3 affinities can be observed. These findings support the assumption that a motif of five amino acids is required for efficient Casp2 inhibition in this class of peptidic, reversible inhibitors. The pentapeptide AcITVKD-CHO (**9**, Casp2 pK_i: 6.40) is the only inhibitor derived from the natural cleavage sequences to show marginal selectivity for Casp2 (twofold selectivity). Interestingly, it does not contain aspartic acid at position P4. A broader series of AcITVKD-CHO analogs including AcITV(Orn) D-CHO (**20**), AcITV(Dab)D-CHO (**23**), AcITV(Dap)D-CHO (**26**), and AcITVKD-CHO (**35**) exhibited moderate selectivity for Casp2. Regarding Casp3 selectivity AcDKVD-CHO (**45**), (Casp2 pK_i: 5.61/5.22; Casp3 pK_i: 7.79), the corresponding tetrapeptide of the recently described AcVDKVD-CHO (Casp2 pK_i: 7.40; Casp3 pK_i: 7.28),[15] showed up as the most selective Casp3 inhibitor in this study with a selectivity factor of 151 or 371, respectively. The associated calculations via molecular modeling are predominantly in agreement with the in vitro data. Crystal structures with bound AcITV(Dab) D-CHO (**23**) in Casp3 confirm that the P4 Thr is a good isostere for

the P4 Asp that induces little change in protein conformation: a good prerequisite for future modeling with the series. In summary, the results of this study provide a vast knowledge of the structure −affinity relationships (SAR) of a large number of peptides with various activities and selectivities within the caspase family. These findings provide a reasonable basis for the development of selective Casp2 inhibitors.

4 | EXPERIMENTAL

4.1 | Chemistry

4.1.1 | General

Unless otherwise listed, chemicals and solvents were purchased from commercial suppliers and used as received. All the solvents were of analytical grade or distilled before use. Dimethylformamide (DMF) and *N*-methyl-2-pyrrolidone (NMP) were purchased from Iris Biotech (Marktredwitz). Sodium borhydride, oxalyl chloride, methanol, dichloromethane, diethyl ether, toluene, ethyl acetate, tetrahydrofuran, and hydrochloric acid 37% were obtained from Fisher Scientific/Acros Organics (Schwerte). If lower concentrations of hydrochloric acid were required, these were diluted accordingly. Isobutyl chloroformate, *tert*-butyl carbazate, *p*-toluenesulfonic acid, *trans*-4-(aminomethyl) cyclohexanecarboxylic acid, *N*,*N*′-diisopropylcarbodiimide (DIC), Oxyma and *N*-methylmorpholine were purchased from TCI (Eschborn). 1-Ethyl-3-(3-dimethylaminopropyl)carbodiimide (EDCI), 1-hydroxybenzotriazole hydrate (HOBt), 1-[bis(dimethylamino)methylene]-1*H*-1,2,3-triazolo [4,5-*b*]pyridinium 3-oxide hexafluorophosphate (HATU), *N*,*N*-diisopropylethylamine (DIPEA), and trifluoroacetic acid (TFA) were obtained from ABCR (Karlsruhe). 1,1'-Carbonyldiimidazole was purchased from Fluorochem (Derbyshire). Aminomethylated polystyrene HL (100–200 mesh), acetic anhydride, and triethylamine were purchased from Merck (Darmstadt). Benzyl alcohol, dimethylsulfoxide, acetic acid, and acetonitrile for high-performance liquid chromatography (HPLC) were obtained from Sigma-Aldrich (Taufkirchen, Germany). Protected amino acids Fmoc-Tyr(*t*Bu)-OH, Fmoc-Arg(Pbf)-OH, Fmoc-Lys(Boc)-OH, Fmoc-Phe-OH, Fmoc-Pro-OH, Fmoc-Val-OH, Fmoc-Asp(O *t*Bu)-OH, Fmoc-Ala-OH, Fmoc-Orn(Boc)-OH, Fmoc-Dab(Boc)-OH, Fmoc-Dap(Boc)-OH, Fmoc-Lys(Ac)-OH, Fmoc-Thr(*t*Bu-OH, Fmoc-Ile-OH, Fmoc-Glu(O*t*Bu)-OH, Fmoc-Gly-OH, Fmoc-Ser(*t*Bu)-OH, Fmoc-Trp(Boc)-OH, Fmoc-Gln-OH, Fmoc-Leu-OH, Fmoc-D-Lys(Boc)-OH and Fmoc-D-Dab(Boc)-OH were procured from Carbolution Chemicals (St. Ingbert). Deuterated solvents for nuclear magnetic resonance (NMR) spectroscopy were purchased from Deutero (Kastellaun). The orbital shaker (Multi Reax) was from Heidolph (Schwabach). The frits had a pore size of 35 µm and were procured from Roland Vetter Laborbedarf (Ammerbuch). The infrared lamp was from Medisana (Neuss), and the thermostat was from PEARL.GmbH (Buggingen). As syringes were used Injekt Luer Solo from Braun (Melsungen). For the preparation of stock solutions, buffers, and HPLC eluents Millipore water was used. NMR spectra (^{1}H NMR, ^{13}C NMR, ^{19}F NMR, DEPT, ^{1}H COSY, HSQC, HMBC) were recorded on a Bruker Avance-300 (7.05 T, ^{1}H: 300 MHz, ^{13}C: 75.5 MHz, ^{19}F: 188) or Avance-400 (9.40T, ^{1}H: 400 MHz, ^{13}C: 100.6 MHz, ^{19}F: 282) NMR spectrometer (Bruker). All chemical shifts are reported in the δ-scale as parts per million (ppm) relative to the solvent's residual peaks as the internal standard. Moreover, the multiplicity, coupling constant (*J*), and the number of protons are stated. Multiplicities are specified with the following abbreviations: s (singlet), d (doublet), t (triplet), q (quartet), quint (quintet), m (multiplet), as well as combinations thereof. High-resolution mass spectrometry (HRMS) was performed on a Q-TOF 6540 ultrahigh definition (UHD) LC/MS system (Agilent Technologies) using an electrospray ionization (ESI) source or on an AccuTOF GCX GC/MS system (Jeol) using an electron ionization (EI) source. Preparative HPLC was performed with a system from Waters (Eschborn) consisting of a Waters 2545 binary gradient module, a Waters 2489 UV/vis-detector, a Waters Fraction Collector 3, and the column was a YMC Triart C18 (150 × 10 mm, 5 µm) (YMC) at a flow rate of 20 ml/min or an HPLC from Knauer consisting of two K-1800 pumps, a K-2001 detector, and the column was a Phenomenex Gemini (250 × 21 mm, 5 µm) (Phenomenex) at a flow rate of 15 ml/min. As a mobile phase, mixtures of MeCN and 0.1% aqueous (aq) TFA were used. The UV detection was carried out at 220 nm. For sample preparation, all compounds were dissolved in a mixture of water/acetonitrile (95/5 v/v) and filtered with PTFE filters (25 mm, 0.2 µm) (Phenomenex). The purified peptides were lyophilized using a CHRIST Alpha 2-4 LD freeze dryer (Osterode am Harz, Germany) equipped with an RZ 6 rotary vane vacuum pump (Vacuubrand). Analytical purity control was performed on an 1100 HPLC system from Agilent Technologies equipped with an Instant Pilot controller, a G1312A binary pump, a G1329A ALS autosampler, a G1379A vacuum degasser, a G1316A column compartment, and a G1315B diode array detector (DAD). The column was a Phenomenex Kinetex XB-C18 column (250 × 4.6 mm 2.5 µm) (Phenomenex) or a Phenomenex Gemini NX-C18 column (250 × 4.6 mm, 5 µm). The oven temperature during HPLC analysis was 30°C. As a mobile phase, mixtures of MeCN/aqueous TFA were used. Absorbance was detected at 220 nm. The injection volume was 20–80 µl at compound concentrations of 1 mM. The following linear gradient was applied: MeCN/TFA (0.05%) (v/v) 0 min: 10:90, 25 min: 95:5, 35 min: 95:5; flow rate: 1.0 ml/min, t_0 (Kinetix XB-C18) = 2.75 min, t_0 (Gemini NX-C18) = 2.99 min (t_0 = dead time). Retention (capacity) factors k were calculated from the retention times t_R according to $k = (t_R - t_0)/t_0$. The purities of the compounds were calculated by the percentage peak area of the chromatograms. The tested compounds have been screened for PAINS and aggregation by publicly available filters (http://zinc15.docking.org/patterns/home, http://advisor.docking.org).[37,38] Compounds have not been previously reported as PAINS or aggregators. None of the data showed abnormalities, for example, high Hill slopes, that could be a hint for PAINS.[38]

The peptides were characterized using the following methods: HRMS, ^{1}H NMR spectroscopy (for spectra, see Supporting Information), and ^{13}C NMR spectroscopy (for spectra, see Supporting Information). Additionally, two-dimensional (2D) NMR spectra like HSQC (for spectra, see Supporting Information) were made. For purity control, HPLC

(RP-HPLC) analysis was performed (for chromatogram, see Supporting Information) with a minimum purity standard of ≥95%.

The InChI codes of the investigated compounds, together with some biological activity data, are provided as Supporting Information.

4.1.2 | General procedure for the synthesis of the peptides

The aspartic acid-loaded semicarbazide amino-Merrifield resin (300 mg, 0.188 mmol, 1 eq) was weighed into a fritted 10 ml syringe. Subsequently, 5 ml of a mixture of piperidine 20% in DMF was drawn up to remove the N-terminal Fmoc protecting group. The syringe was shaken on an orbital shaker at 35°C for 15 min. The orbital shaker was covered with a box, which was insulated from the inside with aluminum foil. An infrared lamp was placed on an aperture on top. To keep the temperature constant at 35°C, the lamp was controlled by a thermostat. The liquid was then removed with the aid of a vacuum flask and the residual resin was washed with DMF (3 × 8 ml). The coupling of the amino acids to the N-terminus was performed by two different methods. The corresponding amino acid (5 eq) and HATU (357 mg, 0.94 mmol, 5 eq) (Method A) or Oxyma (134 mg, 0.94 mmol, 5 eq) (Method B) were weighed in two separate Erlenmeyer flasks. Subsequently, both were dissolved in 3–4 ml of a mixture of DMF/NMP (8/2 v/v). Then *N,N*-diisopropylethylamine (164 µl, 0.94 mmol, 5 eq) (Method A) or *N,N'*-diisopropylcarbodiimide (151 µl, 0.94 mmol, 5 eq) (Method B) was added to the solution of HATU (procedure A)/Oxyma (procedure B). Subsequently, both solutions were drawn up with the resin-loaded syringe and shaken at 35°C for 45 min. The liquid was then removed with the aid of a vacuum flask and the residual resin was washed with DMF (3 × 8 ml).

The coupling and deprotection steps were repeated until the desired tri-, tetra-, or pentapeptide was built up. Then the N-terminal Fmoc protecting group was removed using piperidine in DMF (20%). Subsequently, the N-terminus of the peptide was acetylated by dissolving acetic anhydride (178 µl, 1.88 mmol, 10 eq) and *N,N*-diisopropylethylamine (328 µl, 1.88 mmol, 10 eq) in 6–8 ml DMF. The solution was drawn up with the syringe and shaken for 30 min at room temperature. After completion, the liquid was removed, and the resin was washed with DMF (2 × 8 ml), methanol (2 × 8 ml), dichloromethane (2 × 8 ml), and finally diethyl ether (2 × 8 ml). The peptide was cleaved off the resin, and the side chains were deprotected by drawing up 6 ml of trifluoroacetic acid 90% in water. The syringe was shaken for 1 h at room temperature. The liquid was then poured into a round-bottomed flask. The step was repeated again, and then the cleavage cocktail was diluted with 50 ml water and freeze-dried. The crude product was purified by HPLC, yielding the corresponding peptide.

4.1.2.1 | *(S)-4-(2-Acetamidoacetamido)-5-({(S)-1-[(S)-2-{[(S)-1-carboxy-3-oxopropan-2-yl]carbamoyl}pyrrolidin-1-yl]-3-hydroxy-1-oxopropan-2-yl}amino)-5-oxopentanoic acid (**3**)*

The title compound was synthesized according to the general procedure A, yielding a fluffy white solid (16.7 mg, 17%): RP-HPLC: >99%, (t_R = 3.67, k = 0.22). ^{1}H NMR (400 MHz, D_2O) δ 4.95–4.85 (m, 1H), 4.66–4.60 (m, 1H), 4.42–4.04 (m, 3H), 3.80 (s, 2H), 3.77–3.54 (m, 4H), 2.71–2.38 (m, 2H), 2.35 (t, J = 7.3 Hz, 2H), 2.23–1.94 (m, 2H), 1.93 (s, 3H), 1.91–1.74 (m, 4H). ^{13}C NMR (101 MHz, D_2O) δ 177.05, 175.24, 174.94, 174.27, 173.77, 173.25 (d, J = 3.5 Hz), 171.70, 170.38, 89.67, 60.93, 60.74, 53.51, 52.77, 51.59, 48.09, 42.50, 33.96, 29.89, 29.42, 26.20, 24.46 (d, J = 27.4 Hz), 21.73. *m/z* [M+H$^+$] calculated for $C_{21}H_{32}N_5O_{11}^+$: 530.2093, found 530.2100; $C_{21}H_{31}N_5O_{11}$ (529.50).

4.1.2.2 | *(4S,7S,10S,13S,16S)-4-[(1H-Indol-3-yl)methyl]-7-(carboxymethyl)-16-formyl-10-(3-guanidinopropyl)-13-methyl-2,5,8,11,14-pentaoxo-3,6,9,12,15-pentaazaoctadecan-18-oic acid (**4**)*

The title compound was synthesized according to the general procedure A, yielding a fluffy white solid (12.0 mg, 8%): RP-HPLC: 98%, (t_R = 7.48, k = 1.49). ^{1}H NMR (300 MHz, D_2O) δ 7.50–7.30 (m, 2H), 7.17–6.94 (m, 3H), 4.87 (dd, J = 4.6, 2.7 Hz, 1H), 4.42 (t, J = 6.9 Hz, 1H), 4.34 (t, J = 6.3 Hz, 1H), 4.17–3.91 (m, 3H), 3.09 (d, J = 7.0 Hz, 2H), 2.97 (t, J = 6.8 Hz, 2H), 2.65–2.28 (m, 4H), 1.83 (s, 3H), 1.71–1.46 (m, 2H), 1.45–1.30 (m, 2H), 1.25–1.16 (m, 3H). *m/z* [M+H$^+$] calculated for $C_{30}H_{42}N_9O_{10}$+: 688.3049, found 688.3058; $C_{30}H_{41}N_9O_{10}$ x $C_2HF_3O_2$ (801.73).

4.1.2.3 | *(4S,7S,10S,13S,16S)-4-(3-amino-3-oxopropyl)-7-(carboxymethyl)-16-formyl-13-(3-guanidinopropyl)-10-[(R)-1-hydroxyethyl]-2,5,8,11,14-pentaoxo-3,6,9,12,15-pentaazaoctadecan-18-oic acid (**5**)*

The title compound was synthesized according to the general procedure A, yielding a fluffy white solid (15.0 mg, 10%): RP-HPLC: >99%, (t_R = 3.43, k = 0.14). ^{1}H NMR (300 MHz, D_2O) δ 4.88 (d, J = 2.2 Hz, 1H), 4.24–4.03 (m, 5H), 3.04 (t, J = 6.9 Hz, 2H), 2.90–2.27 (m, 5H), 2.22 (t, J = 7.5 Hz, 2H), 1.98–1.77 (m, 5H), 1.72–1.55 (m, 2H), 1.52–1.39 (m, 2H), 1.04 (d, J = 6.3 Hz, 3H). ^{13}C NMR (75 MHz, D_2O) δ 177.77, 175.19, 174.51, 174.30, 173.64, 173.50, 173.01, 172.68, 171.89, 171.62, 156.72, 89.68, 66.84, 59.33, 53.54, 53.46, 51.51, 50.22, 40.48, 35.21, 31.04, 28.08, 26.70, 25.84, 24.34, 21.64, 18.79. *m/z* [M+H$^+$] calculated for $C_{25}H_{42}N_9O_{12}^+$: 660.2947, found 660.2947; $C_{25}H_{41}N_9O_{12}$ x $C_2HF_3O_2$ (773.68).

4.1.2.4 | *(4S,7S,10S,13S,16S)-7-(carboxymethyl)-16-formyl-10-(3-guanidinopropyl)-13-[(R)-1-hydroxyethyl]-4-methyl-2,5,8,11,14-pentaoxo-3,6,9,12,15-pentaazaoctadecan-18-oic acid (**6**)*

The title compound was synthesized according to the general procedure A, yielding a fluffy white solid (12.2 mg, 9%): RP-HPLC: >99%, (t_R = 3.21, k = 0.07). ^{1}H NMR (300 MHz, D_2O) δ 4.93–4.87 (m, 1H), 4.56–4.49 (m, 1H), 4.28–4.20 (m, 1H), 4.17–3.99 (m, 4H), 3.06 (t, J = 6.8 Hz, 2H), 2.84–2.35 (m, 4H), 1.87 (s, 3H), 1.83–1.59 (m, 2H), 1.54–1.41 (m, 2H), 1.21 (d, J = 7.2 Hz, 3H), 1.09–1.00 (m, 3H). ^{13}C NMR (75 MHz, D_2O) δ 176.37, 175.47, 175.34, 174.61, 174.35, 173.52, 172.54, 171.41, 171.29, 156.72, 89.66, 67.06, 59.47, 53.45, 51.60, 50.23, 50.04, 40.47, 35.44, 34.23, 28.08, 24.30, 21.59, 18.80, 16.30. *m/z* [M+H$^+$] calculated for $C_{23}H_{39}N_8O_{11}^+$: 603.2733, found 603.2741; $C_{23}H_{38}N_8O_{11}$ x $C_2HF_3O_2$ (716.63).

4.1.2.5 | *(S)-3-[(S)-2-Acetamido-4-methylpentanamido]-4-{[(S)-1-((S)-2-{[(S)-1-carboxy-3-oxopropan-2-yl]carbamoyl}pyrrolidin-1-yl)-3-methyl-1-oxobutan-2-yl]amino}-4-oxobutanoic acid (**7**)*

The title compound was synthesized according to the general procedure B, yielding a fluffy white solid (17.4 mg, 55%): RP-HPLC: >99%, (t_R = 9.35, k = 2.12). ^{1}H NMR (300 MHz, D_2O) δ 4.99–4.84 (m, 1H), 4.57 (t, J = 6.8 Hz, 1H), 4.40–3.90 (m, 4H), 3.78–3.31 (m, 2H), 2.90–2.27 (m, 4H), 2.44–2.01 (m, 1H), 2.00–1.63 (m, 7H), 1.54–1.32 (m, 3H), 0.91–0.61 (m, 12H). ^{13}C NMR (75 MHz, D_2O) δ 175.33, 175.21, 174.74, 174.26, 174.01, 173.77, 171.71, 171.66, 171.60, 89.62, 60.77, 57.12, 52.56, 51.51, 51.39, 49.92, 48.25, 39.86, 35.00, 34.05, 33.86, 29.94, 29.66, 29.48, 24.69, 24.54, 24.32, 22.01, 21.59, 20.84, 18.42, 18.34, 17.36. *m/z* [M+H$^+$] calculated for $C_{26}H_{42}N_5O_{10}^+$: 584.2926, found 584.2934; $C_{26}H_{41}N_5O_{10}$ (583.64).

4.1.2.6 | *(S)-3-[(S)-2-Acetamido-3-phenylpropanamido]-4-{[(S)-1-((S)-2-{[(S)-1-carboxy-3-oxopropan-2-yl]carbamoyl}pyrrolidin-1-yl)-3-methyl-1-oxobutan-2-yl]amino}-4-oxobutanoic acid (**8**)*

The title compound was synthesized according to the general procedure A, yielding a fluffy white solid (51.6 mg, 45%): RP-HPLC: >99%, (t_R = 10.04, k = 2.35). ^{1}H NMR (300 MHz, D_2O) δ 7.31–6.93 (m, 5H), 4.91 (dd, J = 5.3, 4.4 Hz, 1H), 4.52–4.35 (m, 2H), 4.27–4.17 (m, 2H), 4.17–3.99 (m, 1H), 3.79–3.24 (m, 2H), 3.06–2.27 (m, 6H), 2.17–2.02 (m, 1H), 2.01–1.62 (m, 7H), 0.90–0.64 (m, 6H). ^{13}C NMR (75 MHz, D_2O) δ 175.32, 175.20, 174.00, 173.88, 173.73, 172.98, 171.79, 171.71, 171.65, 171.43, 136.18, 129.12, 128.78, 127.22, 89.61, 60.79, 57.20, 55.05, 51.51, 51.38, 49.86, 48.27, 36.97, 35.04, 34.06, 33.85, 29.89, 29.64, 29.47, 24.54, 21.60, 18.39, 18.29, 17.51. *m/z* [M+H$^+$] calculated for $C_{29}H_{40}N_5O_{10}$+: 618.2770, found 618.2779; $C_{29}H_{39}N_5O_{10}$ (617.66).

4.1.2.7 | *(4S,7S,10S,13S,16S)-13-(4-Aminobutyl)-4-[(S)-sec-butyl]-16-formyl-7-[(R)-1-hydroxyethyl]-10-isopropyl-2,5,8,11,14-pentaoxo-3,6,9,12,15-pentaazaoctadecan-18-oic acid (**9**)*

The title compound was synthesized according to the general procedure A, yielding a fluffy white solid (30.0 mg, 22%): RP-HPLC: >99%, (t_R = 6.86, k = 1.29). ^{1}H NMR (400 MHz, D_2O) δ 4.94 (t, J = 4.8 Hz, 1H), 4.43–3.94 (m, 6H), 2.88 (t, J = 7.6 Hz, 2H), 2.69–2.32 (m, 2H), 1.94 (s, 4H), 1.80–1.51 (m, 5H), 1.43–1.23 (m, 3H), 1.16–1.03 (m, 4H), 0.90–0.72 (m, 12H). ^{13}C NMR (101 MHz, D_2O) δ 176.01, 175.64, 174.46, 174.24, 173.15, 172.91, 171.64, 171.57, 89.74, 67.14, 59.46, 58.98, 58.71, 53.59, 51.66, 39.20, 36.18, 34.62, 30.68, 30.12, 26.27, 24.64, 21.95, 21.66, 18.86, 18.43, 17.84, 14.88, 10.32. *m/z* [M+H$^+$] calculated for $C_{27}H_{49}N_6O_9$+: 601.3556, found 601.2558; $C_{27}H_{48}N_6O_9$ x $C_2HF_3O_2$ (714.74).

4.1.2.8 | *(4S,7S,10S,13S)-4-(Carboxymethyl)-13-formyl-7-(3-guanidinopropyl)-10-methyl-2,5,8,11-tetraoxo-3,6,9,12-tetraazapentadecan-15-oic acid (**10**)*

The title compound was synthesized according to the general procedure B, yielding a fluffy white solid (17.6 mg, 15%): RP-HPLC: >99%, (t_R = 3.66, k = 0.22). ^{1}H NMR (400 MHz, D_2O) δ 4.93 (t, J = 3.8 Hz, 1H), 4.56 (d, J = 6.7 Hz, 1H), 4.28–4.07 (m, 3H), 3.10 (t, J = 6.9 Hz, 2H), 2.87–2.37 (m, 4H), 1.92 (s, 3H), 1.84–1.44 (m, 4H), 1.30–1.20 (m, 3H). ^{13}C NMR (101 MHz, D_2O) δ 175.30, 175.23, 174.66, 174.51, 174.25, 174.16, 173.03, 172.98, 172.90, 172.80, 156.79, 89.72, 53.35, 53.20, 51.49, 50.24, 49.89, 49.83, 40.51, 35.38, 34.12, 34.07, 28.08, 27.98, 24.31, 21.72, 16.81, 16.64. *m/z* [M+H$^+$] calculated for $C_{19}H_{32}N_7O_9^+$: 502.2257, found 502.2256; $C_{19}H_{31}N_7O_9$ x $C_2HF_3O_2$ (615.52).

4.1.2.9 | *(S)-3-{(S)-2-[(S)-2-Acetamido-5-guanidinopentanamido]propanamido}-4-oxobutanoic acid (**11**)*

The title compound was synthesized according to the general procedure B, yielding a fluffy white solid (9.6 mg, 10%): RP-HPLC: >99%, (t_R = 3.74, k = 0.25). ^{1}H NMR (400 MHz, D_2O) δ 4.94 (dd, J = 4.5, 3.0 Hz, 1H), 4.28–4.05 (m, 3H), 3.10 (t, J = 6.8 Hz, 2H), 2.72–2.36 (m, 2H), 1.94–1.88 (m, 3H), 1.78–1.46 (m, 4H), 1.35–1.19 (m, 3H). ^{13}C NMR (101 MHz, D_2O) δ 175.34, 175.30, 174.66, 174.50, 174.42, 174.36, 173.56, 156.80, 89.72, 53.44, 53.33, 51.51, 49.77, 49.68, 40.57, 34.18, 28.22, 24.27, 21.65, 16.83, 16.67. *m/z* [M+H$^+$] calculated for $C_{15}H_{27}N_6O_6$+: 387.1987, found 387.1985; $C_{15}H_{26}N_6O_6$ x $C_2HF_3O_2$ (500.43).

4.1.2.10 | *(4S,7S,10S,13S)-4-(Carboxymethyl)-13-formyl-10-(3-guanidinopropyl)-7-[(R)-1-hydroxyethyl]-2,5,8,11-tetraoxo-3,6,9,12-tetraazapentadecan-15-oic acid (**12**)*

The title compound was synthesized according to the general procedure B, yielding a fluffy white solid (26.2 mg, 22%): RP-HPLC: >99%, (t_R = 3.75, k = 0.25). ^{1}H NMR (400 MHz, D_2O) δ 4.92 (dd, J = 4.6, 2.3 Hz, 1H), 4.35–4.04 (m, 4H), 3.15–3.04 (m, 2H), 2.89–2.37 (m, 4H), 1.94 (s, 3H), 1.84–1.39 (m, 4H), 1.14–1.05 (m, 3H). ^{13}C NMR (101 MHz, D_2O) δ 175.24, 175.17, 174.40, 174.24, 173.21, 173.13, 173.05, 171.66, 171.57, 156.77, 89.71, 89.66, 66.89, 59.23, 59.13, 53.54, 53.48, 51.54, 51.51, 50.24, 40.50, 35.41, 34.21, 33.99, 28.33, 28.12, 24.35, 24.31, 21.76, 18.78. *m/z* [M+H$^+$] calculated for $C_{20}H_{34}N_7O_{10}^+$: 532.2362, found 532.2366; $C_{20}H_{33}N_7O_{10}$ x $C_2HF_3O_2$ (645.55).

4.1.2.11 | *(S)-3-{(S)-2-[(2S,3R)-2-Acetamido-3-hydroxybutanamido]-5-guanidinopentanamido}-4-oxobutanoic acid (**13**)*

The title compound was synthesized according to the general procedure B, yielding a fluffy white solid (16.0 mg, 16%): RP-HPLC: >99%, (t_R = 3.36, k = 0.22). ^{1}H NMR (400 MHz, D_2O) δ 4.98–4.90 (m, 1H), 4.32–4.21 (m, 1H), 4.19–4.00 (m, 2H), 3.17–3.02 (m, 2H), 2.73–2.34 (m, 2H), 2.05–1.88 (m, 3H), 1.83–1.43 (m, 4H), 1.32–1.04 (m, 3H). *m/z* [M+H$^+$] calculated for $C_{16}H_{29}N_6O_7^+$: 417.2092, found 417.2093; $C_{16}H_{28}N_6O_7$ x $C_2HF_3O_2$ (530.46).

4.1.2.12 | *(4S,7S,10S,13S)-4-(Carboxymethyl)-13-formyl-7-(3-guanidinopropyl)-10-[(R)-1-hydroxyethyl]-2,5,8,11-tetraoxo-3,6,9,12-tetraazapentadecan-15-oic acid (**14**)*

The title compound was synthesized according to the general procedure B, yielding a fluffy white solid (17.4 mg, 14%): RP-HPLC: 97%, (t_R = 3.62, k = 0.21). ^{1}H NMR (300 MHz, D_2O) δ 4.90 (dd, J = 4.6,

1.6 Hz, 1H), 4.53 (t, *J* = 6.2 Hz, 1H), 4.36–3.93 (m, 4H), 3.06 (t, *J* = 6.9 Hz, 2H), 2.84–2.35 (m, 4H), 1.87 (s, 3H), 1.82–1.38 (m, 5H), 1.11–0.97 (m, 3H). *m/z* [M+H$^+$] calculated for $C_{20}H_{34}N_7O_{10}^+$: 532.2362, found 532.2364; $C_{20}H_{33}N_7O_{10}$ x $C_2HF_3O_2$ (645.55).

4.1.2.13 | *(S)-3-{(2S,3R)-2-[(S)-2-acetamido-5-guanidinopentanamido]-3-hydroxybutanamido}-4-oxobutanoic acid (**15**)*

The title compound was synthesized according to the general procedure B, yielding a fluffy white solid (5.3 mg, 5%): RP-HPLC: >99%, (t_R = 3.60, *k* = 0.20). ^{1}H NMR (400 MHz, D_2O) δ 4.97–4.91 (m, 1H), 4.30–4.01 (m, 4H), 3.11 (t, *J* = 6.8 Hz, 2H), 2.73–2.39 (m, 2H), 1.93 (s, 3H), 1.77–1.61 (m, 2H), 1.60–1.48 (m, 2H), 1.16–1.01 (m, 3H). *m/z* [M+H$^+$] calculated for $C_{16}H_{29}N_6O_7^+$: 417.2092, found 417.2096; $C_{16}H_{28}N_6O_7$ x $C_2HF_3O_2$ (530.46).

4.1.2.14 | *(S)-3-Acetamido-4-{[(S)-1-((S)-2-{[(S)-1-carboxy-3-oxopropan-2-yl]carbamoyl}pyrrolidin-1-yl)-3-methyl-1-oxobutan-2-yl]amino}-4-oxobutanoic acid (**16**)*

The title compound was synthesized according to the general procedure A, yielding a fluffy white solid (41.7 mg, 47%): RP-HPLC: 99%, (t_R = 6.17, *k* = 1.06). ^{1}H NMR (400 MHz, D_2O) δ 5.01–4.89 (m, 1H), 4.61–4.55 (m, 1H), 4.37–4.31 (m, 1H), 4.30–4.19 (m, 1H), 4.18–4.04 (m, 1H), 3.83–3.29 (m, 2H), 2.87–2.34 (m, 4H), 2.28–2.06 (m, 1H), 2.05–1.69 (m, 7H), 0.90–0.73 (m, 6H). ^{13}C NMR (101 MHz, D_2O) δ 175.36, 175.24, 174.18, 173.96, 173.79, 172.38, 171.84, 171.77, 171.69, 89.65, 60.83, 60.80, 57.08, 57.01, 51.55, 51.43, 50.12, 48.34, 35.39, 34.08, 33.92, 30.08, 30.03, 29.69, 29.52, 24.68, 24.56, 21.69, 18.42, 18.35, 17.30, 17.28. *m/z* [M+H$^+$] calculated for $C_{20}H_{31}N_4O_9^+$: 471.2086, found 471.2093; $C_{20}H_{30}N_4O_9$ (470.48).

4.1.2.15 | *(S)-3-[(S)-1-(Acetyl-L-valyl)pyrrolidine-2-carboxamido]-4-oxobutanoic acid (**17**)*

The title compound was synthesized according to the general procedure A, yielding a fluffy white solid (26.2 mg, 39%): RP-HPLC: >99%, (t_R = 6.66, *k* = 1.22). ^{1}H NMR (400 MHz, D_2O) δ 4.98–4.92 (m, 1H), 4.35–4.19 (m, 2H), 4.17–4.03 (m, 1H), 3.85–3.72 (m, 1H), 3.64–3.34 (m, 1H), 2.71–2.34 (m, 2H), 2.24–2.08 (m, 1H), 2.04–1.68 (m, 7H), 0.94–0.75 (m, 6H). ^{13}C NMR (101 MHz, D_2O) δ 175.37, 175.26, 174.21, 173.87, 172.51, 172.44, 172.36, 89.65, 60.86, 60.82, 57.30, 57.24, 51.56, 51.43, 48.31, 34.10, 33.92, 29.76, 29.69, 29.65, 29.48, 24.75, 24.61, 21.51, 18.35, 18.28, 17.36. *m/z* [M+H$^+$] calculated for $C_{16}H_{26}N_3O_5^+$: 356.1816, found 356.1821; $C_{16}H_{25}N_3O_5$ (355.39).

4.1.2.16 | *(4S,7S,10S,13S)-10-(4-Aminobutyl)-13-formyl-4-[(R)-1-hydroxyethyl]-7-isopropyl-2,5,8,11-tetraoxo-3,6,9,12-tetraazapentadecan-15-oic acid (**18**)*

The title compound was synthesized according to the general procedure B, yielding a fluffy white solid (18.8 mg, 25%): RP-HPLC: >99%, (t_R = 3.45, *k* = 0.15). ^{1}H NMR (300 MHz, D_2O) δ 4.89 (dd, *J* = 4.6, 2.0 Hz, 1H), 4.21–3.91 (m, 5H), 2.83 (t, *J* = 7.6 Hz, 2H), 2.72–2.33 (m, 2H), 2.00–1.81 (m, 4H), 1.73–1.47 (m, 4H), 1.38–1.17 (m, 2H), 1.05 (d, *J* = 6.4 Hz, 3H), 0.79 (t, *J* = 6.5 Hz, 6H). *m/z* [M+H$^+$] calculated for $C_{21}H_{38}N_5O_8^+$: 488.2715, found 488.2724; $C_{21}H_{37}N_5O_8$ x $C_2HF_3O_2$ (601.58).

4.1.2.17 | *(S)-3-{(S)-2-[(S)-2-Acetamido-3-methylbutanamido]−6-aminohexanamido}-4-oxobutanoic acid (**19**)*

The title compound was synthesized according to the general procedure B, yielding a fluffy white solid (20.0 mg, 32%): RP-HPLC: >99%, (t_R = 3.50, *k* = 0.17).^{1}H NMR (300 MHz, D_2O) δ 4.88 (dd, *J* = 4.6, 2.3 Hz, 1H), 4.25–3.82 (m, 3H), 2.83 (t, *J* = 7.6 Hz, 2H), 2.70–2.30 (m, 2H), 1.96–1.80 (m, 4H), 1.75–1.46 (m, 4H), 1.39–1.15 (m, 2H), 0.80 (t, *J* = 5.5 Hz, 6H). ^{13}C NMR (75 MHz, D_2O) δ 206.60, 175.42, 174.44, 173.77, 173.27, 173.16, 89.66, 59.77, 53.50, 51.51, 39.17, 34.28, 30.51, 29.91, 26.19, 21.96, 21.56, 18.33, 17.75. *m/z* [M+H$^+$] calculated for $C_{17}H_{31}N_4O_6$+: 387.2238, found 387.2243; $C_{17}H_{30}N_4O_6$ x $C_2HF_3O_2$ (500.47).

4.1.2.18 | *(4S,7S,10S,13S,16S)-13-(3-Aminopropyl)-4-[(S)-sec-butyl]−16-formyl-7-[(R)-1-hydroxyethyl]-10-isopropyl-2,5,8,11,14-pentaoxo-3,6,9,12,15-pentaazaoctadecan-18-oic acid (**20**)*

The title compound was synthesized according to the general procedure A, yielding a fluffy white solid (42.2 mg, 48%): RP-HPLC: >99%, (t_R = 7.07, *k* = 1.36). ^{1}H NMR (300 MHz, D_2O) δ 4.92–4.84 (m, 1H), 4.40–3.85 (m, 6H), 2.85 (t, *J* = 7.2 Hz, 2H), 2.68–2.28 (m, 2H), 2.00–1.79 (m, 4H), 1.77–1.23 (m, 6H), 1.13–0.95 (m, 3H), 0.86–0.64 (m, 12H). ^{13}C NMR (75 MHz, D_2O) δ 206.59, 175.94, 175.48, 174.45, 174.23, 172.96, 172.56, 171.65, 89.67, 67.12, 59.60, 58.92, 58.69, 53.15, 51.59, 38.85, 36.13, 34.56, 30.07, 28.16, 24.62, 23.20, 21.63, 18.83, 18.40, 17.86, 14.84, 10.29. *m/z* [M+H$^+$] calculated for $C_{26}H_{47}N_6O_9^+$: 587.3399, found 587.3410; $C_{26}H_{46}N_6O_9$ x $C_2HF_3O_2$ (700.71).

4.1.2.19 | *(4S,7S,10S,13S)-10-(3-Aminopropyl)-13-formyl-4-[(R)-1-hydroxyethyl]-7-isopropyl-2,5,8,11-tetraoxo-3,6,9,12-tetraazapentadecan-15-oic acid (**21**)*

The title compound was synthesized according to the general procedure B, yielding a fluffy white solid (21.9 mg, 30%): RP-HPLC: >99%, (t_R = 3.46, *k* = 0.15). ^{1}H NMR (300 MHz, D_2O) δ 4.88 (dd, *J* = 4.6, 3.1 Hz, 1H), 4.40–3.88 (m, 5H), 2.85 (t, *J* = 6.1 Hz, 2H), 2.69–2.32 (m, 2H), 1.98–1.81 (m, 4H), 1.75–1.47 (m, 4H), 1.05 (d, *J* = 6.4 Hz, 3H), 0.78 (t, *J* = 6.7 Hz, 6H). *m/z* [M+H$^+$] calculated for $C_{20}H_{36}N_5O_8^+$: 474.2558, found 474.2561; $C_{20}H_{35}N_5O_8$ x $C_2HF_3O_2$ (587.55).

4.1.2.20 | *(S)-3-{(S)-2-[(S)-2-Acetamido-3-methylbutanamido]-5-aminopentanamido}-4-oxobutanoic acid (**22**)*

The title compound was synthesized according to the general procedure B, yielding a fluffy white solid (36.3 mg, 60%): RP-HPLC: >99%, (t_R = 3.43, *k* = 0.14). ^{1}H NMR (300 MHz, D_2O) δ 4.92–4.82 (m, 1H), 4.27–4.18 (m, 1H), 4.15–4.03 (m, 1H), 3.92–3.79 (m, 1H), 2.85 (t, *J* = 7.0 Hz, 2H), 2.69–2.27 (m, 2H), 1.96–1.80 (m, 4H), 1.78–1.44 (m, 4H), 0.78 (t, *J* = 6.8 Hz, 6H). ^{13}C NMR (75 MHz, D_2O) δ 206.60, 175.17, 174.52, 173.82, 172.65, 89.66, 59.93, 53.05, 51.51,

38.85, 34.32, 29.89, 28.12, 23.22, 21.55, 18.37, 17.81. *m/z* [M+H$^+$] calculated for $C_{16}H_{29}N_4O_6^+$: 373.2082, found 373.2084; $C_{16}H_{28}N_4O_6$ x $C_2HF_3O_2$ (486.45).

4.1.2.21 | *(4S,7S,10S,13S,16S)-13-(2-Aminoethyl)-4-[(S)-sec-butyl]-16-formyl-7-[(R)-1-hydroxyethyl]-10-isopropyl-2,5,8,11,14-pentaoxo-3,6,9,12,15-pentaazaoctadecan-18-oic acid (**23**)*

The title compound was synthesized according to the general procedure A, yielding a fluffy white solid (41.0 mg, 48%): RP-HPLC: >99%, (t_R = 7.11, k = 1.37). ^{1}H NMR (300 MHz, D_2O) δ 4.89 (t, J = 4.9 Hz, 1H), 4.38–3.88 (m, 6H), 2.97–2.82 (m, 2H), 2.70–2.30 (m, 2H), 2.10–1.84 (m, 6H), 1.77–1.25 (m, 2H), 1.04 (d, J = 6.4 Hz, 3H), 0.84–0.68 (m, 12H). ^{13}C NMR (75 MHz, D_2O) δ 175.69, 175.26, 174.47, 174.26, 173.13, 172.10, 171.69, 171.55, 89.64, 67.13, 59.61, 58.84, 58.72, 51.57, 51.10, 36.18, 36.12, 34.52, 30.07, 29.04, 24.62, 21.63, 18.83, 18.37, 17.88, 14.84, 10.30. *m/z* [M+H$^+$] calculated for $C_{25}H_{45}N_6O_9^+$: 573.3243, found 573.3246; $C_{25}H_{44}N_6O_9$ x $C_2HF_3O_2$ (686.68).

4.1.2.22 | *(4S,7S,10S,13S)-10-(2-Aminoethyl)-13-formyl-4-[(R)-1-hydroxyethyl]-7-isopropyl-2,5,8,11-tetraoxo-3,6,9,12-tetraazapentadecan-15-oic acid (**24**)*

The title compound was synthesized according to the general procedure B, yielding a fluffy white solid (18.2 mg, 25%): RP-HPLC: >99%, (t_R = 3.44, k = 0.15). ^{1}H NMR (300 MHz, D_2O) δ 4.89 (t, J = 4.7 Hz, 1H), 4.40–3.90 (m, 5H), 2.99–2.80 (m, 2H), 2.70–2.30 (m, 2H), 2.06–1.84 (m, 6H), 1.05 (d, J = 6.4 Hz, 3H), 0.83–0.75 (m, 6H). *m/z* [M+H$^+$] calculated for $C_{19}H_{34}N_5O_8^+$: 460.2402, found 460.2412; $C_{19}H_{33}N_5O_8$ x $C_2HF_3O_2$ (573.52).

4.1.2.23 | *(S)-3-{(S)-2-[(S)-2-Acetamido-3-methylbutanamido]-4-aminobutanamido}-4-oxobutanoic acid (**25**)*

The title compound was synthesized according to the general procedure B, yielding a fluffy white solid (8.9 mg, 15%): RP-HPLC: 96%, (t_R = 3.53, k = 0.18). ^{1}H NMR (400 MHz, D_2O) δ 4.95 (d, J = 4.8 Hz, 1H), 4.44–4.29 (m, 1H), 4.18–4.10 (m, 1H), 3.92 (d, J = 7.3 Hz, 1H), 3.04–2.86 (m, 2H), 2.72–2.37 (m, 2H), 2.16–2.01 (m, 1H), 2.02–1.86 (m, 5H), 0.89–0.75 (m, 6H). ^{13}C NMR (101 MHz, D_2O) δ 175.06, 174.65, 174.20, 174.01, 172.20, 171.66, 89.68, 59.99, 51.54, 51.07, 36.27, 34.37, 29.86, 28.99, 21.57, 18.37, 17.84. *m/z* [M+H$^+$] calculated for $C_{15}H_{27}N_4O_6^+$: 359.1925, found 359.1930; $C_{15}H_{26}N_4O_6$ x $C_2HF_3O_2$ (472.42).

4.1.2.24 | *(4S,7S,10S,13S,16S)-13-(Aminomethyl)-4-[(S)-sec-butyl]-16-formyl-7-[(R)-1-hydroxyethyl]-10-isopropyl-2,5,8,11,14-pentaoxo-3,6,9,12,15-pentaazaoctadecan-18-oic acid (**26**)*

The title compound was synthesized according to the general procedure A, yielding a fluffy white solid (24.2 mg, 29%): RP-HPLC: >99%, (t_R = 7.01, k = 1.34). ^{1}H NMR (300 MHz, D_2O) δ 4.91 (dd, J = 8.1, 4.6 Hz, 1H), 4.64–4.57 (m, 1H), 4.50–3.92 (m, 5H), 3.41–3.05 (m, 2H), 2.77–2.27 (m, 2H), 2.02–1.85 (m, 4H), 1.76–1.23 (m, 2H), 1.05 (d, J = 6.4 Hz, 3H), 0.86–0.68 (m, 12H). ^{13}C NMR (75 MHz, D_2O) δ 175.48, 174.95, 174.92, 174.52, 174.36, 173.56, 173.39, 171.91, 171.87, 169.73, 169.26, 89.56, 67.16, 67.01, 59.53, 58.81, 58.71, 58.12, 51.64, 51.52, 50.80, 50.57, 40.02, 36.08, 35.93, 34.40, 30.16, 29.89, 24.65, 24.52, 21.62, 21.51, 18.81, 18.37, 18.35, 17.73, 17.71, 17.69, 14.84, 14.68, 10.29, 10.12. *m/z* [M+H$^+$] calculated for $C_{24}H_{43}N_6O_9^+$: 559.3086, found 559.3093; $C_{24}H_{42}N_6O_9$ x $C_2HF_3O_2$ (672.66).

4.1.2.25 | *(4S,7S,10S,13S)-10-(Aminomethyl)-13-formyl-4-[(R)-1-hydroxyethyl]-7-isopropyl-2,5,8,11-tetraoxo-3,6,9,12-tetraazapentadecan-15-oic acid (**27**)*

The title compound was synthesized according to the general procedure B, yielding a fluffy white solid (14.6 mg, 21%): RP-HPLC: >99%, (t_R = 3.44, k = 0.15). ^{1}H NMR (300 MHz, D_2O) δ 4.91 (dd, J = 8.4, 4.6 Hz, 1H), 4.63–4.51 (m, 1H), 4.27–3.86 (m, 4H), 3.41–3.04 (m, 4H), 2.73–2.29 (m, 1H), 2.02–1.82 (m, 4H), 1.06 (d, J = 6.4 Hz, 3H), 0.89–0.74 (m, 6H). *m/z* [M+H$^+$] calculated for $C_{18}H_{32}N_5O_8^+$: 446.2245, found 446.2253; $C_{18}H_{31}N_5O_8$ x $C_2HF_3O_2$ (559.50).

4.1.2.26 | *(S)-3-{(S)-2-[(S)-2-Acetamido-3-methylbutanamido]-3-aminopropanamido}-4-oxobutanoic acid (**28**)*

The title compound was synthesized according to the general procedure B, yielding a fluffy white solid (20.2 mg, 35%): RP-HPLC: >99%, (t_R = 3.45, k = 0.15). ^{1}H NMR (300 MHz, D_2O) δ 4.94–4.86 (m, 1H), 4.64–4.54 (m, 1H), 4.20–3.82 (m, 2H), 3.40–3.06 (m, 2H), 2.73–2.32 (m, 2H), 2.02–1.84 (m, 4H), 0.87–0.75 (m, 6H). ^{13}C NMR (75 MHz, D_2O) δ 206.61, 175.36, 174.90, 174.79, 174.22, 169.41, 89.58, 59.88, 51.47, 50.45, 40.02, 34.31, 29.89, 21.58, 18.31, 17.66. *m/z* [M+H$^+$] calculated for $C_{14}H_{25}N_4O_6^+$: 345.1769, found 345.1776; $C_{14}H_{24}N_4O_6$ x $C_2HF_3O_2$ (458.39).

4.1.2.27 | *(4S,7S,10S,13S,16S)-13-(4-Acetamidobutyl)-4-[(S)-sec-butyl]-16-formyl-7-[(R)-1-hydroxyethyl]-10-isopropyl-2,5,8,11,14-pentaoxo-3,6,9,12,15-pentaazaoctadecan-18-oic acid (**29**)*

The title compound was synthesized according to the general procedure A, yielding a fluffy white solid (26.0 mg, 39%): RP-HPLC: >99%, (t_R = 8.20, k = 1.73). ^{1}H NMR (400 MHz, D_2O) δ 4.93 (d, J = 4.7 Hz, 1H), 4.32–4.24 (m, 1H), 4.22–3.95 (m, 5H), 3.08–3.00 (m, 2H), 2.73–2.36 (m, 3H), 2.04–1.90 (m, 4H), 1.86 (s, 3H), 1.78–1.52 (m, 2H), 1.45–1.32 (m, 2H), 1.30–1.17 (m, 2H), 1.07 (d, J = 6.5 Hz, 3H), 0.89–0.69 (m, 12H). ^{13}C NMR (75 MHz, DMSO-d_6) δ 206.43, 175.40, 175.40, 172.16, 171.93, 171.92, 171.88, 171.04, 169.47, 169.47, 102.87, 66.89, 58.57, 58.01, 57.50, 52.83, 38.75, 36.85, 33.48, 29.22, 24.84, 23.30, 23.05, 22.89, 20.05, 19.54, 18.28, 15.84, 11.44. *m/z* [M+H$^+$] calculated for $C_{29}H_{51}N_6O_{10}^+$: 643.3661, found 643.3670; $C_{29}H_{50}N_6O_{10}$ (642.75).

4.1.2.28 | *(4S,7S,10S,13S)-10-(4-Acetamidobutyl)-13-formyl-4-[(R)-1-hydroxyethyl]-7-isopropyl-2,5,8,11-tetraoxo-3,6,9,12-tetraazapentadecan-15-oic acid (**30**)*

The title compound was synthesized according to the general procedure A, yielding a fluffy white solid (25.8 mg, 39%): RP-HPLC: >99%, (t_R = 5.74, k = 0.91). ^{1}H NMR (300 MHz, D_2O) δ 4.88

(d, J = 4.7 Hz, 1H), 4.20–3.87 (m, 5H), 2.99 (t, J = 2.0 Hz, 2H), 2.79–2.30 (m, 2H), 1.95–1.85 (m, 4H), 1.81 (s, 3H), 1.69–1.48 (m, 2H), 1.40–1.29 (m, 2H), 1.25–1.12 (m, 2H), 1.03 (d, J = 6.4 Hz, 3H), 0.78 (dd, J = 6.8, 4.6 Hz, 6H). ^{13}C NMR (75 MHz, D_2O) δ 175.20, 175.11, 174.52, 173.93, 173.41, 173.29, 173.01, 172.09, 89.66, 67.10, 59.55, 59.42, 56.09, 53.69, 51.48, 39.15, 34.07, 30.74, 30.11, 27.70, 22.36, 21.86, 21.69, 18.86, 18.39, 17.77. m/z [M+H$^+$] calculated for $C_{23}H_{40}N_4O_9^+$: 530.2821, found 530.2825; $C_{23}H_{39}N_4O_9$ (529.59).

4.1.2.29 | *(S)-3-{(S)-6-Acetamido-2-[(S)-2-acetamido-3-methylbutanamido]hexanamido}-4-oxobutanoic acid (**31**)*

The title compound was synthesized according to the general procedure A, yielding a fluffy white solid (32.6 mg, 61%): RP-HPLC: >99%, (t_R = 5.50, k = 0.83). ^{1}H NMR (300 MHz, D_2O) δ 4.88 (d, J = 5.0 Hz, 1H), 4.24–4.01 (m, 2H), 3.95–3.86 (m, 1H), 3.00 (t, J = 6.7 Hz, 2H), 2.72–2.28 (m, 2H), 1.96–1.85 (m, 4H), 1.81 (s, 3H), 1.71–1.47 (m, 2H), 1.43–1.29 (m, 2H), 1.27–1.10 (m, 2H), 0.79 (dd, J = 6.8, 3.2 Hz, 6H). ^{13}C NMR (75 MHz, D_2O) δ 206.61, 175.14, 175.07, 174.43, 173.93, 173.66, 173.37, 89.66, 59.82, 53.60, 51.47, 39.14, 34.05, 30.67, 29.96, 27.70, 22.34, 21.84, 21.61, 18.39, 18.32, 17.68, 17.66. m/z [M+H$^+$] calculated for $C_{19}H_{31}N_4O_7^+$: 427.2198, found 427.2202; $C_{19}H_{30}N_4O_7$ (428.49).

4.1.2.30 | *(4S,7S,13S,16S)-13-(4-Aminobutyl)-4-[(S)-sec-butyl]-16-formyl-7-[(R)-1-hydroxyethyl]-2,5,8,11,14-pentaoxo-3,6,9,12,15-pentaazaoctadecan-18-oic acid (**32**)*

The title compound was synthesized according to the general procedure B, yielding a fluffy white solid (25.4 mg, 30%): RP-HPLC: 98%, (t_R = 5.81, k = 0.94). ^{1}H NMR (300 MHz, D_2O) δ 4.86 (d, J = 4.2 Hz, 1H), 4.44–3.99 (m, 5H), 3.90–3.72 (m, 2H), 2.83 (t, J = 7.4 Hz, 2H), 2.47–2.16 (m, 1H), 1.89 (s, 3H), 1.78–1.17 (m, 9H), 1.07 (d, J = 6.4 Hz, 4H), 0.80–0.68 (m, 6H). ^{13}C NMR (75 MHz, D_2O) δ 206.60, 174.62, 174.40, 173.18, 172.39, 172.30, 170.80, 170.34, 90.02, 67.08, 59.17, 58.73, 58.48, 53.58, 52.39, 42.57, 42.40, 39.19, 36.02, 30.84, 26.25, 24.58, 21.81, 21.66, 18.71, 14.86, 10.31. m/z [M+H$^+$] calculated for $C_{24}H_{43}N_6O_9^+$: 559.3086, found 559.3088; $C_{24}H_{42}N_6O_9$ x $C_2HF_3O_2$ (672.66).

4.1.2.31 | *(4S,10S,13S)-10-(4-Aminobutyl)-13-formyl-4-[(R)-1-hydroxyethyl]-2,5,8,11-tetraoxo-3,6,9,12-tetraazapentadecan-15-oic acid (**33**)*

The title compound was synthesized according to the general procedure B, yielding a fluffy white solid (27.5 mg, 39%): RP-HPLC: >99%, (t_R = 3.08, k = 0.12). ^{1}H NMR (300 MHz, D_2O) δ 4.92–4.85 (m, 1H), 4.31–4.02 (m, 4H), 3.89–3.72 (m, 2H), 2.83 (t, J = 7.5 Hz, 2H), 2.73–2.29 (m, 2H), 1.95 (s, 3H), 1.73–1.47 (m, 4H), 1.32–1.04 (m, 5H). m/z [M+H$^+$] calculated for $C_{18}H_{32}N_5O_8^+$: 446.2245, found 446.2251; $C_{18}H_{31}N_5O_8$ x $C_2HF_3O_2$ (559.50).

4.1.2.32 | *(S)-3-{(S)-2-[2-Acetamidoacetamido]-6-aminohexanamido}-4-oxobutanoic acid (**34**)*

The title compound was synthesized according to the general procedure B, yielding a fluffy white solid (35.1 mg, 41%): RP-HPLC: >99%, (t_R = 2.58, k = −0.14). ^{1}H NMR (400 MHz, D_2O) δ 4.92 (t, J = 4.6 Hz, 1H), 4.35–4.01 (m, 2H), 3.89–3.71 (m, 2H), 2.91–2.81 (m, 2H), 2.74–2.56 (m, 1H), 2.54–2.30 (m, 1H), 1.93 (s, 3H), 1.88–1.47 (m, 4H), 1.44–1.17 (m, 2H). ^{13}C NMR (101 MHz, D_2O) δ 175.51, 175.25, 175.23, 175.01, 174.92, 173.60, 171.68, 89.67, 53.61, 53.57, 52.33, 51.57, 51.52, 42.55, 42.46, 39.22, 34.22, 33.99, 29.97, 26.22, 26.13, 22.02, 21.69. m/z [M+H$^+$] calculated for $C_{14}H_{25}N_4O_6^+$: 345.1769, found 345.1769; $C_{14}H_{24}N_4O_6$ x $C_2HF_3O_2$ (458.39).

4.1.2.33 | *(4S,7S,10S,13S,16S)-13-(4-Aminobutyl)-4-[(S)-sec-butyl]-16-formyl-7-[(R)-1-hydroxyethyl]-10-methyl-2,5,8,11,14-pentaoxo-3,6,9,12,15-pentaazaoctadecan-18-oic acid (**35**)*

The title compound was synthesized according to the general procedure B, yielding a fluffy white solid (26.9 mg, 31%): RP-HPLC: 96%, (t_R = 5.98, k = 0.99). ^{1}H NMR (300 MHz, D_2O) δ 4.90–4.81 (m, 1H), 4.32–3.83 (m, 6H), 2.84 (t, J = 7.4 Hz, 2H), 2.73–1.98 (m, 2H), 1.88 (s, 3H), 1.75–1.45 (m, 5H), 1.37–1.21 (m, 5H), 1.05 (d, J = 6.4 Hz, 4H), 0.80–0.66 (m, 6H). ^{13}C NMR (75 MHz, D_2O) δ 206.60, 178.81, 174.71, 174.51, 174.37, 174.31, 173.24, 173.13, 171.48, 171.29, 90.08, 67.26, 67.11, 58.83, 58.72, 53.84, 53.70, 52.48, 49.76, 49.57, 39.18, 36.08, 30.75, 30.49, 26.27, 24.62, 21.83, 21.64, 18.81, 16.56, 14.84, 10.27. m/z [M+H$^+$] calculated for $C_{25}H_{45}N_6O_9$+: 573.3243, found 573.3246; $C_{25}H_{44}N_6O_9$ x $C_2HF_3O_2$ (686.68).

4.1.2.34 | *(4S,7S,10S,13S)-10-(4-Aminobutyl)-13-formyl-4-[(R)-1-hydroxyethyl]-7-methyl-2,5,8,11-tetraoxo-3,6,9,12-tetraazapentadecan-15-oic acid (**36**)*

The title compound was synthesized according to the general procedure B, yielding a fluffy white solid (17.6 mg, 24%): RP-HPLC: >99%, (t_R = 3.09, k = 0.11). ^{1}H NMR (300 MHz, D_2O) δ 4.88 (dd, J = 4.6, 1.9 Hz, 1H), 4.33–3.94 (m, 5H), 2.83 (t, J = 7.5 Hz, 2H), 2.73–2.25 (m, 2H), 2.01–1.88 (m, 3H), 1.75–1.45 (m, 4H), 1.36–1.03 (m, 8H). m/z [M+H$^+$] calculated for $C_{19}H_{34}N_5O_8^+$: 460.2402, found 460.2408; $C_{19}H_{33}N_5O_8$ x $C_2HF_3O_2$ (573.52).

4.1.2.35 | *(S)-3-{(S)-2-[(S)-2-Acetamidopropanamido]-6-aminohexanamido}-4-oxobutanoic acid (**37**)*

The title compound was synthesized according to the general procedure B, yielding a fluffy white solid (46.2 mg, 52%): RP-HPLC: >99%, (t_R = 3.25, k = 0.19). ^{1}H NMR (400 MHz, D_2O) δ 4.92 (dd, J = 4.6, 2.5 Hz, 1H), 4.33–4.02 (m, 3H), 2.87 (t, J = 6.0 Hz, 2H), 2.73–2.58 (m, 1H), 2.51–2.33 (m, 1H), 1.89 (s, 3H), 1.86–1.48 (m, 4H), 1.43–1.18 (m, 5H). ^{13}C NMR (101 MHz, D_2O) δ 175.51, 175.44, 175.36, 175.25, 175.16, 174.22, 174.09, 173.52, 173.45, 89.65, 53.50, 52.27, 51.49, 49.79, 49.72, 39.23, 34.14, 33.95, 29.95, 26.20, 26.11, 22.01, 21.54, 16.45. m/z [M+H$^+$] calculated for $C_{15}H_{27}N_4O_6^+$: 359.1925, found 359.1929; $C_{15}H_{26}N_4O_6$ x $C_2HF_3O_2$ (472.42).

4.1.2.36 | *(4S,7S,10S,13S,16S)-13-(4-Aminobutyl)-16-formyl-7-[(R)-1-hydroxyethyl]-10-isopropyl-4-methyl-2,5,8,11,14-pentaoxo-3,6,9,12,15-pentaazaoctadecan-18-oic acid (**38**)*

The title compound was synthesized according to the general procedure A, yielding a fluffy white solid (35.8 mg, 28%): RP-HPLC:

>99%, (t_R = 3.98, k = 0.33). ^{1}H NMR (400 MHz, D_2O) δ 4.93 (dd, J = 4.6, 2.3 Hz, 1H), 4.33–3.90 (m, 6H), 2.87 (t, J = 7.6 Hz, 2H), 2.75–2.35 (m, 2H), 2.01–1.86 (m, 4H), 1.79–1.46 (m, 4H), 1.33–1.18 (m, 5H), 1.08 (d, J = 6.4 Hz, 3H), 0.82 (t, J = 6.3 Hz, 6H). ^{13}C NMR (101 MHz, D_2O) δ 175.73, 175.27, 175.08, 174.28, 173.73, 173.23, 173.13, 173.02, 171.87, 171.81, 89.70, 67.11, 59.63, 59.49, 58.98, 53.63, 53.54, 51.51, 49.92, 49.89, 39.20, 34.19, 33.89, 30.63, 30.57, 30.17, 30.11, 26.24, 22.00, 21.96, 21.61, 18.86, 18.41, 18.36, 17.85, 17.81, 16.55. m/z [M+H$^+$] calculated for $C_{24}H_{43}N_6O_9^+$: 559.3086, found 559.3093; $C_{24}H_{42}N_6O_9$ x $C_2HF_3O_2$ (672.66).

4.1.2.37 | *(4S,7S,10S,13S,16S)-13-(2-Aminoethyl)-16-formyl-7-[(R)-1-hydroxyethyl]-10-isopropyl-4-methyl-2,5,8,11,14-pentaoxo-3,6,9,12,15-pentaazaoctadecan-18-oic acid (**39**)*

The title compound was synthesized according to the general procedure A, yielding a fluffy white solid (32.5 mg, 27%): RP-HPLC: >99%, (t_R = 3.68, k = 0.23). ^{1}H NMR (400 MHz, D_2O) δ 4.97–4.91 (m, 1H), 4.44–4.30 (m, 1H), 4.30–4.04 (m, 4H), 4.11–3.94 (m, 1H), 3.03–2.86 (m, 2H), 2.75–2.36 (m, 2H), 2.22–1.84 (m, 6H), 1.32–1.23 (m, 3H), 1.09 (d, J = 6.4 Hz, 3H), 0.89–0.78 (m, 6H). ^{13}C NMR (101 MHz, D_2O) δ 175.80, 175.34, 175.02, 174.33, 173.29, 171.97, 171.76, 89.59, 67.13, 59.60, 58.90, 51.58, 51.23, 49.94, 36.18, 33.90, 30.09, 29.12, 21.61, 18.86, 18.34, 17.86, 16.54. m/z [M+H$^+$] calculated for $C_{22}H_{39}N_6O_9^+$: 531.2773, found 531.2782; $C_{22}H_{38}N_6O_9$ x $C_2HF_3O_2$ (644.60).

4.1.2.38 | *(4S,7S,10S,13S,16S)-4-[(S)-sec-Butyl]-16-formyl-7-[(R)-1-hydroxyethyl]-13-(hydroxymethyl)-10-isopropyl-2,5,8,11,14-pentaoxo-3,6,9,12,15-pentaazaoctadecan-18-oic acid (**40**)*

The title compound was synthesized according to the general procedure A, yielding a fluffy white solid (36.7 mg, 36%): RP-HPLC: 99%, (t_R = 8.30, k = 1.77). ^{1}H NMR (400 MHz, D_2O) δ 4.95 (d, J = 4.4 Hz, 1H), 4.41–4.23 (m, 2H), 4.22–3.98 (m, 4H), 3.81–3.62 (m, 2H), 2.73–2.35 (m, 2H), 2.07–1.85 (m, 4H), 1.81–1.67 (m, 2H), 1.47–1.27 (m, 1H), 1.19–0.99 (m, 4H), 0.88–0.69 (m, 12H). m/z [M+H$^+$] calculated for $C_{24}H_{42}N_5O_{10}^+$: 560.2926, found 560.2932; $C_{24}H_{41}N_5O_{10}$ (559.62).

4.1.2.39 | *(4S,7S,10S,13S,16S)-7-(Carboxymethyl)-16-formyl-13-(hydroxymethyl)-4,10-diisopropyl-2,5,8,11,14-pentaoxo-3,6,9,12,15-pentaazaoctadecan-18-oic acid (**41**)*

The title compound was synthesized according to the general procedure A, yielding a fluffy white solid (45.2 mg, 43%): RP-HPLC: >99%, (t_R = 7.17, k = 1.39). ^{1}H NMR (400 MHz, D_2O) δ 4.94 (d, J = 4.5 Hz, 1H), 4.65–4.64 (m, 1H), 4.39–4.28 (m, 1H), 4.19–3.89 (m, 3H), 3.87–3.64 (m, 2H), 3.07–2.38 (m, 4H), 2.11–1.87 (m, 5H), 0.90–0.76 (m, 12H). ^{13}C NMR (101 MHz, D_2O) δ 175.25, 175.17, 174.51, 174.18, 173.62, 173.36, 173.32, 172.35, 172.31, 171.18, 171.10, 89.65, 61.18, 61.09, 59.78, 59.66, 55.81, 55.62, 51.59, 50.08, 35.19, 34.09, 33.95, 29.94, 21.65, 18.45, 18.34, 17.61, 17.44. m/z [M+H$^+$] calculated for $C_{23}H_{38}N_5O_{11}^+$: 560.2562, found 560.2572; $C_{23}H_{37}N_5O_{11}$ (559.57).

4.1.2.40 | *(4S,7S,10S,13S)−4-(Carboxymethyl)−13-formyl-7-isopropyl-10-methyl-2,5,8,11-tetraoxo-3,6,9,12-tetraazapentadecan-15-oic acid (**42**)*

The title compound was synthesized according to the general procedure A, yielding a fluffy white solid (45.5 mg, 55%): RP-HPLC: >99%, (t_R = 5.36, k = 0.79). ^{1}H NMR (400 MHz, D_2O) δ 4.93 (dd, J = 4.5, 3.0 Hz, 1H), 4.61 (t, J = 6.8 Hz, 1H), 4.27–4.07 (m, 2H), 4.11–3.94 (m, 1H), 2.87–2.35 (m, 4H), 2.05–1.92 (m, 1H), 1.91 (s, 3H), 1.32–1.19 (m, 3H), 0.87–0.75 (m, 6H). ^{13}C NMR (101 MHz, D_2O) δ 175.27, 175.15, 174.97, 174.56, 174.40, 174.18, 174.08, 172.89, 172.80, 172.70, 89.69, 59.48, 59.30, 51.46, 50.13, 49.79, 35.32, 34.06, 33.89, 30.23, 30.13, 21.69, 18.42, 18.36, 17.43, 16.82, 16.70. m/z [M+H$^+$] calculated for $C_{18}H_{29}N_4O_9^+$: 445.1929, found 445.1933; $C_{18}H_{28}N_4O_9$ (444.44).

4.1.2.41 | *(S)-3-{(S)-2-[(S)-2-Acetamido-3-methylbutanamido]propanamido}-4-oxobutanoic acid (**43**)*

The title compound was synthesized according to the general procedure A, yielding a fluffy white solid (35.8 mg, 58%): RP-HPLC: >99%, (t_R = 5.37, k = 0.79). ^{1}H NMR (400 MHz, D_2O) δ 4.93 (dd, J = 4.6, 2.2 Hz, 1H), 4.30–4.05 (m, 2H), 4.00–3.93 (m, 1H), 2.71–2.37 (m, 2H), 2.02–1.88 (m, 4H), 1.33–1.21 (m, 3H), 0.83 (dd, J = 6.8, 3.0 Hz, 6H). ^{13}C NMR (101 MHz, D_2O) δ 175.28, 175.18, 174.59, 174.52, 174.42, 173.65, 173.49, 89.70, 89.67, 59.67, 59.52, 51.48, 51.45, 49.74, 49.65, 34.09, 33.95, 30.08, 30.02, 21.66, 18.38, 17.53, 16.85, 16.73. m/z [M+H$^+$] calculated for $C_{14}H_{24}N_3O_6^+$: 330.1660, found 330.1666; $C_{14}H_{23}N_3O_6$ (329.35).

4.1.2.42 | *(4S,7S,10S,13S)-10-(4-Aminobutyl)-4-(carboxymethyl)-13-formyl-7-isopropyl-2,5,8,11-tetraoxo-3,6,9,12-tetraazapentadecan-15-oic acid (**44**)*

The title compound was synthesized according to the general procedure B, yielding a fluffy white solid (42.4 mg, 37%): RP-HPLC: >99%, (t_R = 3.77, k = 0.26). ^{1}H NMR (400 MHz, D_2O) δ 4.92 (dd, J = 4.6, 1.5 Hz, 1H), 4.59 (t, J = 6.4 Hz, 1H), 4.27–4.06 (m, 2H), 4.04–3.94 (m, 1H), 2.86 (t, J = 7.6 Hz, 2H), 2.85–2.35 (m, 4H), 2.02–1.85 (m, 4H), 1.77–1.48 (m, 4H), 1.40–1.18 (m, 2H), 0.86–0.75 (m, 6H). ^{13}C NMR (101 MHz, D_2O) δ 175.24, 175.07, 174.18, 174.06, 173.77, 173.38, 173.28, 173.18, 173.15, 172.71, 172.63, 89.69, 59.65, 59.51, 53.62, 53.56, 51.49, 50.15, 39.22, 35.33, 34.18, 33.88, 30.57, 30.45, 30.14, 30.07, 26.21, 26.18, 22.00, 21.95, 21.70, 18.43, 18.40, 17.62. m/z [M+H$^+$] calculated for $C_{21}H_{36}N_5O_9^+$: 502.2508, found 502.2513; $C_{21}H_{35}N_5O_9$ x $C_2HF_3O_2$ (615.56).

4.1.2.43 | *(4S,7S,10S,13S)-7-(4-Aminobutyl)-4-(carboxymethyl)-13-formyl-10-isopropyl-2,5,8,11-tetraoxo-3,6,9,12-tetraazapentadecan-15-oic acid (**45**)*

The title compound was synthesized according to the general procedure B, yielding a fluffy white solid (47.6 mg, 41%): RP-HPLC: >99%, (t_R = 3.67, k = 0.22). ^{1}H NMR (400 MHz, D_2O) δ 4.91 (dd, J = 6.4, 4.8 Hz, 1H), 4.55 (t, J = 6.8 Hz, 1H), 4.28–4.20 (m, 1H), 4.20–4.08 (m, 1H), 3.95 (d, J = 7.9 Hz, 1H), 2.87 (t, J = 7.6 Hz, 2H), 2.83–2.36 (m, 4H), 1.99–1.84 (m, 4H), 1.78–1.47 (m, 4H), 1.39–1.19

(m, 2H), 0.88–0.72 (m, 6H). ^{13}C NMR (101 MHz, D_2O) δ 175.25, 175.15, 174.22, 173.98, 173.66, 173.45, 173.38, 172.99, 172.88, 172.71, 172.68, 172.63, 172.57, 89.81, 89.69, 59.73, 53.50, 53.44, 51.58, 51.50, 50.21, 39.22, 35.41, 34.08, 33.92, 30.26, 30.15, 30.11, 26.21, 21.98, 21.93, 21.72, 18.39, 18.33, 18.29, 17.71, 17.65. *m/z* [M+H$^+$] calculated for $C_{21}H_{36}N_5O_9^+$: 502.2508, found 502.2514; $C_{21}H_{35}N_5O_9$ x $C_2HF_3O_2$ (615.56).

4.1.2.44 | *(4S,7S,10S,13S)-10-(2-Aminoethyl)-4-(carboxymethyl)-13-formyl-7-isopropyl-2,5,8,11-tetraoxo-3,6,9,12-tetraazapentadecan-15-oic acid (**46**)*

The title compound was synthesized according to the general procedure A, yielding a fluffy white solid (76.1 mg, 69%): RP-HPLC: 99%, (t_R = 3.68, k = 0.23). ^{1}H NMR (400 MHz, D_2O) δ 4.93 (t, J = 4.7 Hz, 1H), 4.59 (t, J = 6.4 Hz, 1H), 4.39–4.30 (m, 1H), 4.17–4.09 (m, 1H), 4.04–3.94 (m, 1H), 3.00–2.86 (m, 2H), 2.84–2.37 (m, 4H), 2.13–1.87 (m, 6H), 0.87–0.77 (m, 6H). ^{13}C NMR (101 MHz, D_2O) δ 175.26, 174.98, 174.21, 174.12, 173.41, 173.36, 172.81, 172.78, 171.77, 171.63, 89.66, 89.59, 59.69, 59.62, 51.55, 51.51, 51.24, 51.14, 50.13, 36.24, 35.34, 34.29, 33.87, 30.00, 29.04, 28.92, 21.69, 18.40, 18.38, 17.69, 17.65. *m/z* [M+H$^+$] calculated for $C_{19}H_{32}N_5O_9^+$: 474.2195, found 474.2200; $C_{19}H_{31}N_5O_9$ x $C_2HF_3O_2$ (587.51).

4.1.2.45 | *(4S,7S,10S,13R,16S)-13-(4-Aminobutyl)-4-[(S)-sec-butyl]-16-formyl-7-[(R)-1-hydroxyethyl]-10-isopropyl-2,5,8,11,14-pentaoxo-3,6,9,12,15-pentaazaoctadecan-18-oic acid (**47**)*

The title compound was synthesized according to the general procedure A (using 150 mg resin), yielding a fluffy white solid (27.3 mg, 41%): RP-HPLC: 99%, (t_R = 6.85, k = 1.28). ^{1}H NMR (400 MHz, D_2O) δ 4.91 (t, J = 4.5 Hz, 1H), 4.32–4.25 (m, 1H), 4.22–3.82 (m, 5H), 2.87 (t, J = 7.7 Hz, 2H), 2.75–2.32 (m, 2H), 2.04–1.78 (m, 4H), 1.84–1.50 (m, 5H), 1.46–1.22 (m, 3H), 1.20–1.00 (m, 4H), 0.92–0.70 (m, 12H). ^{13}C NMR (101 MHz, D_2O) δ 175.57, 174.58, 174.36, 174.28, 173.39, 173.35, 173.19, 171.76, 171.60, 89.80, 67.07, 59.94, 59.80, 58.93, 58.86, 58.78, 53.68, 53.61, 51.70, 51.62, 39.17, 36.16, 30.67, 30.28, 30.06, 29.93, 26.25, 26.20, 24.66, 22.15, 22.11, 21.68, 18.86, 18.82, 18.42, 17.88, 17.84, 14.88, 10.34. *m/z* [M+H$^+$] calculated for $C_{27}H_{49}N_6O_9^+$: 601.3556, found 601.3564; $C_{27}H_{48}N_6O_9$ x $C_2HF_3O_2$ (714.74).

4.1.2.46 | *(4S,7S,10S,13R,16S)-13-(2-Aminoethyl)-4-[(S)-sec-butyl]-16-formyl-7-[(R)-1-hydroxyethyl]-10-isopropyl-2,5,8,11,14-pentaoxo-3,6,9,12,15-pentaazaoctadecan-18-oic acid (**48**)*

The title compound was synthesized according to the general procedure A (using 150 mg resin), yielding a fluffy white solid (27.0 mg, 42%): RP-HPLC: >99%, (t_R = 6.63, k = 1.21). ^{1}H NMR (400 MHz, D_2O) δ 4.95–4.91 (m, 1H), 4.41–4.23 (m, 2H), 4.22–3.83 (m, 4H), 3.07–2.87 (m, 2H), 2.77–2.34 (m, 2H), 2.22–2.03 (m, 1H), 2.03–1.86 (m, 5H), 1.82–1.68 (m, 1H), 1.45–1.31 (m, 1H), 1.22–0.98 (m, 4H), 0.92–0.73 (m, 12H). ^{13}C NMR (101 MHz, D_2O) δ 175.46, 175.36, 174.59, 174.42, 174.35, 173.47, 173.39, 171.85, 171.73, 89.76, 67.10, 59.97, 58.89, 58.83, 51.65, 51.34, 36.38, 36.14, 34.43, 29.88, 29.80, 29.03, 24.68, 21.68, 18.82, 18.40, 17.89, 14.88, 10.33. *m/z* [M+H$^+$] calculated for $C_{25}H_{45}N_6O_9^+$: 573.3243, found 573.3250; $C_{25}H_{44}N_6O_9$ x $C_2HF_3O_2$ (686.68).

4.1.2.47 | *(4S,7S,10S,13R,16S)-13-(4-Aminobutyl)-7-(carboxymethyl)-16-formyl-4,10-diisopropyl-2,5,8,11,14-pentaoxo-3,6,9,12,15-pentaazaoctadecan-18-oic acid (**49**)*

The title compound was synthesized according to the general procedure A (using 150 mg resin), yielding a fluffy white solid (23.2 mg, 35%): RP-HPLC: >99%, (t_R = 5.89, k = 0.96). ^{1}H NMR (400 MHz, D_2O) δ 4.91 (dd, J = 8.1, 4.6 Hz, 1H), 4.67–4.59 (m, 1H), 4.24–4.08 (m, 2H), 3.99–3.86 (m, 2H), 2.95–2.34 (m, 6H), 2.06–1.75 (m, 5H), 1.83–1.48 (m, 4H), 1.41–1.17 (m, 2H), 0.91–0.76 (m, 12H). ^{13}C NMR (101 MHz, D_2O) δ 175.66, 175.52, 175.50, 174.76, 174.73, 174.65, 174.62, 173.78, 173.69, 173.46, 172.62, 172.59, 172.48, 89.78, 60.10, 60.02, 59.93, 59.91, 53.73, 53.66, 51.66, 51.60, 50.35, 50.28, 39.19, 35.62, 34.33, 34.23, 30.55, 30.34, 29.86, 26.18, 22.14, 21.68, 18.46, 18.41, 18.32, 17.68, 17.64, 17.60. *m/z* [M+H$^+$] calculated for $C_{26}H_{45}N_6O_{10}^+$: 601.3192, found 601.3203; $C_{26}H_{44}N_6O_{10}$ x $C_2HF_3O_2$ (714.69).

4.1.2.48 | *(4S,7S,10S,13R,16S)-13-(2-Aminoethyl)-7-(carboxymethyl)-16-formyl-4,10-diisopropyl-2,5,8,11,14-pentaoxo-3,6,9,12,15-pentaazaoctadecan-18-oic acid (**50**)*

The title compound was synthesized according to the general procedure A (using 150 mg resin), yielding a fluffy white solid (25.7 mg, 40%): RP-HPLC: >99%, (t_R = 5.79, k = 0.93). ^{1}H NMR (400 MHz, D_2O) δ 4.93 (t, J = 4.7 Hz, 1H), 4.65–4.61 (m, 1H), 4.38–4.30 (m, 1H), 4.20–4.11 (m, 1H), 4.00–3.86 (m, 2H), 2.99–2.38 (m, 6H), 2.20–1.86 (m, 7H), 0.88–0.77 (m, 12H). ^{13}C NMR (101 MHz, D_2O) δ 175.24, 175.19, 174.36, 174.26, 173.81, 173.74, 173.65, 173.61, 172.52, 172.33, 171.97, 171.90, 89.73, 60.15, 60.03, 59.95, 51.63, 51.60, 51.40, 50.13, 50.08, 36.39, 35.17, 34.22, 34.03, 29.87, 29.69, 29.65, 28.89, 28.72, 21.67, 18.45, 18.31, 17.67. *m/z* [M+H$^+$] calculated for $C_{24}H_{41}N_6O_{10}^+$: 573.2879, found 573.2888; $C_{24}H_{40}N_6O_{10}$ x $C_2HF_3O_2$ (686.64).

4.1.2.49 | *(4S,7S,10R,13S,16S)-10-(4-Aminobutyl)-7-(carboxymethyl)-16-formyl-4,13-diisopropyl-2,5,8,11,14-pentaoxo-3,6,9,12,15-pentaazaoctadecan-18-oic acid (**51**)*

The title compound was synthesized according to the general procedure A (using 150 mg resin), yielding a fluffy white solid (32.1 mg, 48%): RP-HPLC: >99%, (t_R = 6.11, k = 1.04). ^{1}H NMR (400 MHz, D_2O) δ 4.92 (d, J = 4.7 Hz, 1H), 4.67–4.59 (m, 1H), 4.30–3.87 (m, 4H), 3.02–2.37 (m, 6H), 2.06–1.87 (m, 5H), 1.83–1.48 (m, 4H), 1.40–1.23 (m, 2H), 0.89–0.71 (m, 12H). ^{13}C NMR (101 MHz, D_2O) δ 175.28, 175.22, 174.95, 174.10, 173.93, 173.57, 172.91, 172.87, 172.34, 172.28, 89.79, 60.18, 59.73, 59.68, 53.82, 51.60, 50.34, 50.22, 39.18, 35.58, 35.49, 34.09, 34.02, 30.54, 30.50, 30.18, 30.01, 29.76, 26.15, 22.07, 21.75, 18.43, 18.40, 18.36, 18.31, 17.66. *m/z* [M+H$^+$] calculated for $C_{26}H_{45}N_6O_9^+$: 601.3192, found 601.3203; $C_{26}H_{44}N_6O_9$ x $C_2HF_3O_2$ (714.69).

4.1.2.50 | *(4S,7S,10R,13S,16S)-10-(2-Aminoethyl)-7-(carboxymethyl)-16-formyl-4,13-diisopropyl-2,5,8,11,14-pentaoxo-3,6,9,12,15-pentaazaoctadecan-18-oic acid (**52**)*

The title compound was synthesized according to the general procedure A (using 150 mg resin), yielding a fluffy white solid (29.8 mg, 46%): RP-HPLC: >99%, (t_R = 6.07, k = 1.02). ^{1}H NMR (400 MHz, D_2O) δ 4.95–4.91 (m, 1H), 4.60 (t, J = 6.9 Hz, 1H), 4.40–4.31 (m, 1H), 4.23–4.11 (m, 1H), 4.03–3.87 (m, 2H), 3.03–2.91 (m, 2H), 2.90–2.39 (m, 4H), 2.22–2.06 (m, 1H), 2.06–1.88 (m, 6H), 0.87–0.75 (m, 12H). ^{13}C NMR (101 MHz, D_2O) δ 175.33, 175.27, 174.99, 174.27, 174.05, 172.80, 172.76, 172.66, 172.63, 172.04, 172.01, 89.75, 60.21, 59.96, 59.86, 51.63, 51.59, 51.57, 51.52, 50.51, 36.37, 35.50, 34.10, 29.99, 29.92, 29.76, 28.86, 21.76, 18.28, 17.71. *m/z* [M+H$^+$] calculated for $C_{24}H_{41}N_6O_{10}^+$: 573.2879, found 573.2888; $C_{24}H_{40}N_6O_{10}$ x $C_2HF_3O_2$ (686.64).

4.1.2.51 | *(4S,7S,10R,13S,16S)-10-(4-Aminobutyl)-7-(carboxymethyl)-16-formyl-4-isopropyl-13-methyl-2,5,8,11,14-pentaoxo-3,6,9,12,15-pentaazaoctadecan-18-oic acid (**53**)*

The title compound was synthesized according to the general procedure A (using 150 mg resin), yielding a fluffy white solid (24.6 mg, 38%): RP-HPLC: 99%, (t_R = 4.80, k = 0.60). ^{1}H NMR (400 MHz, D_2O) δ 4.93 (dd, J = 7.6, 4.6 Hz, 1H), 4.64–4.58 (m, 1H), 4.24–4.07 (m, 3H), 3.93 (d, J = 7.0 Hz, 1H), 2.93–2.37 (m, 6H), 2.02–1.90 (m, 4H), 1.83–1.48 (m, 4H), 1.42–1.20 (m, 5H), 0.88–0.79 (m, 6H). ^{13}C NMR (101 MHz, D_2O) δ 175.25, 174.93, 174.56, 174.50, 174.10, 174.01, 173.53, 173.34, 172.47, 89.76, 60.12, 53.81, 53.76, 51.55, 51.50, 50.41, 50.38, 49.88, 39.18, 35.46, 35.38, 34.20, 34.13, 30.28, 29.76, 26.15, 22.02, 21.73, 18.28, 17.63, 16.95, 16.78. *m/z* [M+H$^+$] calculated for $C_{24}H_{41}N_6O_{10}^+$: 573.2879, found 573.2887; $C_{24}H_{40}N_6O_{10}$ x $C_2HF_3O_2$ (686.64).

4.1.2.52 | *(4S,7S,10R,13S,16S)-10-(2-Aminoethyl)-7-(carboxymethyl)-16-formyl-4-isopropyl-13-methyl-2,5,8,11,14-pentaoxo-3,6,9,12,15-pentaazaoctadecan-18-oic acid (**54**)*

The title compound was synthesized according to the general procedure A (using 150 mg resin), yielding a fluffy white solid (18.0 mg, 29%): RP-HPLC: 99%, (t_R = 4.71, k = 0.57). ^{1}H NMR (400 MHz, D_2O) δ 4.96–4.90 (m, 1H), 4.61–4.54 (m, 1H), 4.36–4.24 (m, 1H), 4.24–4.08 (m, 2H), 3.93 (d, J = 7.0 Hz, 1H), 3.01–2.90 (m, 2H), 2.89–2.37 (m, 4H), 2.20–2.07 (m, 1H), 2.05–1.88 (m, 5H), 1.32–1.22 (m, 3H), 0.88–0.77 (m, 6H). ^{13}C NMR (101 MHz, D_2O) δ 175.27, 175.23, 174.96, 174.48, 174.45, 174.13, 172.71, 172.69, 171.95, 171.82, 171.80, 89.75, 60.14, 51.52, 51.46, 50.51, 50.06, 36.37, 35.21, 34.10, 29.77, 28.65, 21.72, 18.26, 17.68, 16.90, 16.73. *m/z* [M+H$^+$] calculated for $C_{22}H_{37}N_6O_{10}^+$: 545.2566, found 545.2576; $C_{22}H_{36}N_6O_{10}$ x $C_2HF_3O_2$ (658.59).

4.1.2.53 | *(4S,7S,10S,13S,16S)-7-(Carboxymethyl)-16-formyl-4,10-bis[(R)-1-hydroxyethyl]-13-methyl-2,5,8,11,14-pentaoxo-3,6,9,12,15-pentaazaoctadecan-18-oic acid (**55**)*

The title compound was synthesized according to the general procedure B, yielding a fluffy white solid (9.3 mg, 9%): RP-HPLC: >99%, (t_R = 3.75, k = 0.25). ^{1}H NMR (400 MHz, D_2O) δ 4.92 (t, J = 4.7 Hz, 1H), 4.78–4.68 (m, 1H), 4.33–3.94 (m, 6H), 3.24–2.29 (m, 4H), 2.03–1.92 (m, 3H), 1.40–1.00 (m, 9H). ^{13}C NMR (101 MHz, D_2O) δ 175.24, 175.21, 174.78, 174.57, 174.50, 174.24, 172.68, 172.57, 172.16, 171.41, 171.31, 89.71, 67.00, 59.40, 59.25, 56.19, 51.51, 50.15, 49.91, 35.17, 34.08, 21.75, 18.82, 16.83, 16.65. *m/z* [M+H$^+$] calculated for $C_{21}H_{39}N_5O_{12}^+$: 548.2198, found 548.2198; $C_{21}H_{38}N_5O_{12}$ (547.52).

4.2 | Molecular modeling

Covalent docking studies were performed using the "Covalent Docking (CovDock)" module within the Schrödinger small-molecule drug discovery software suite (Schrödinger, LLC, Version 2021.3 unless otherwise noted. The crystal structures of Casp2 (PDBid: 1pyo) and Casp3 (PDBid: 3edq) were prepared using the module "Protein Preparation Wizard" in Maestro with the default protein parameters. Hydrogen atoms were added and water molecules that were beyond 5 Å from heterocyclic groups were deleted. The covalently bound ligands AcLDESD-CHO:1pyo, AcLDESD-CHO:3edq where D-CHO represents "aspartic acid aldehyde" were included in the protein structures during their preparation for the covalent docking. In the experiments below, the protein structures prepared in this fashion are denoted by PP:PDBid, for example, PP:1pyo. Hydrogen bonds were optimized, the partial charges were assigned, and the protein structure was energy-minimized using OPLS3e force field.[39] Following this preparation, the covalent bond connecting the ligand to the protein was broken and the now-separated aldehyde (reactive functional group) and cysteine (nucleophilic reaction group) were reconstituted by adjusting bond orders, adding hydrogens, and minimizing these groups in place. This free ligand (the "Workspace Ligand") was employed to create the covalent docking grid used in the covalent docking and scoring (vide infra). The individual target receptors were set up using the following reactive cysteine residues (A:155, 1pyo; A:163, 3edq). The "Reaction Type" SMARTS string {[H]C=O} was built as a customized nucleophilic addition to a double bond. The "Box Center" for the docking grid was set using the "Centroid of (the) Workspace Ligand." Docking was performed in the "Pose Prediction (Thorough)" mode. A "Minimization radius" of 3.0 Å was used, "Perform MM-GBSA scoring" was selected, and three (3) "Output poses per ligand reaction site" were selected (only the lowest energy pose is reported). Ligands for covalent docking experiments were drawn in ChemDraw, imported into Maestro as sdf, and refined into 3D structures using the "Ligand Preparation" module and its default parameters. These 3D structures, with the appropriate tautomers and charges, were directly used in "Covalent Docking" experiments and are designated as PL:ligand name, for example, PL:AcLDESD-CHO. "Cdock Affinity" is reported in kcal/mol. Five starting points for cdock affinity prediction were created by the following protocol. These are structures **1–5** (state number) in Figure 3. (**1**) Standard input as described above; (**2**) Prime (module in the Schrödinger small-molecule drug discovery

software suite) minimization of state **1**; **(3–5)** states selected from 433 states generated by searching of the conformational space of for example, AcVDVAD-CHO with a 10 kcal/mol energy window (**3** = lowest energy state, **4** = middle energy state, and **5** = highest energy state).

4.3 | Fluorometric enzyme assay

The expression and purification of recombinant Casp, circularly permutated caspase-2 (cpCasp2), and recombinant caspase-3 were performed as previously described by Bresinsky et al.[15]

4.3.1 | 384-Well protocol

Compound affinity for caspases was measured in fluorometric assays. Casp2, cpCasp2, and Casp3 were produced in-house as described below. Human recombinant Casp1, Casp6, Casp7, and Casp9 were purchased from BioVision (Milpitas). AFC fluorogenic substrates and control peptides (AcYVAD-CHO, AcVDVAD-CHO, AcDEVD-CHO, AcVEID-CHO, and AcLEHD-CHO) were purchased from Bachem (Torrance). K_m values were determined experimentally to be the following: Casp1: 5.9 µM; Casp2: 37.1 µM; cpCasp2: 89.2 µM; Casp3: 7.6 µM; Casp6: 43.1 µM; Casp7: 13.8 µM; Casp9: 149.1 µM. Enzymes were diluted in buffer: 100 mM MES (pH 6.5) for Casp2 and cpCasp2 or 100 mM HEPES (pH 7.0) for all other caspases, plus 150 mM NaCl, 0.1% CHAPS, 1.5% sucrose, 10 mM DTT. Enzyme concentrations were 0.05 U/well for Casp1, Casp6, and Casp7; 0.5 U/well for Casp9, 20 nM/well for Casp2 and cpCasp2; and 2 nM/well for Casp3. The enzyme in buffer (19 µl) was added per well in a black 384-well Corning 4514 assay plate. Test compounds were serially diluted in dimethyl sulfoxide (DMSO) and plated in duplicate into a Corning 3656 transfer plate. The test compound was added to assay plates in 0.5 µl aliquots per well and mixed 10 times using a BiomekFX (Beckman Coulter). The compound and enzyme mixture was incubated at 37°C for 5 min for reversible inhibitors. The BiomekFX was then used to add and mix 0.5 µl of the AFC substrate in DMSO from a Corning 3656 transfer plate (final assay concentrations: 5 µM AcYVAD-AFC for Casp1, 10 µM Z-VDVAD-AFC for Casp2 and cpCasp2, 5 µM AcDEVD-AFC for Casp3, 5 µM Z-VEID-AFC for Casp6, 5 µM AcDEVD-AFC for Casp7, and 34 µM AcLEHD-AFC for Casp9) to the assay plate for a total assay volume of 20 µl. Fluorescence from free AFC was read at 37°C every 5 min over an hour using a CLARIOstar (BMG Labtech) plate reader (λ_{ex} = 400 nm, λ_{em} = 505 nm). The 40 min time point was reported, consistent with the reported literature.[40–43]

4.3.2 | 96-Well protocol (Casp2/3)

Compound affinity for caspases was measured in fluorometric assays. Casp2, cpCasp2, and Casp3 were produced in-house as described below. AFC fluorogenic substrates Z-VDVAD-AFC and AcDEVD-AFC and control peptides AcVDVAD-CHO and AcDEVD-CHO were purchased from Bachem (Torrance). Enzyme was diluted in buffer: 100 mM MES (pH 6.5) for Casp2 and cpCasp2 or 100 mM HEPES (pH 7.0) for Casp3, plus 150 mM NaCl, 0.1% CHAPS, 1.5% sucrose, and 10 mM DTT. Enzyme concentrations were 5 nM/well for Casp2 and cpCasp2; and 2 nM/well for Casp3. Enzyme in buffer (96.5 µl) was added per well in a black Corning 3356 96-well assay plate. Test compounds were serially DMSO and plated in triplicate in a Corning 3357 transfer plate. The test compound was added to assay plates in 1 µl aliquots per well and mixed 10 times using a BiomekFX (Beckman Coulter). The compound and enzyme mixture was incubated at 37°C for 5 min. The BiomekFX was then used to add and mix 2.5 µl of the AFC substrate in DMSO from a transfer plate (final assay concentrations: 25 µM Z-VDVAD-AFC for Casp2 and cpCasp2, 10 µM AcDEVD-AFC for Casp3) to the assay plate for a total assay volume of 100 µl in the assay plate. Fluorescence from free AFC was read at 37°C every 5 min over an hour using a CLARIOstar (BMG Labtech) plate reader (λ_{ex} = 400 nm, λ_{em} = 505 nm). The 40 min time point was reported, consistent with the reported literature.[40–43]

4.4 | Crystallography

4.4.1 | Casp3 crystallography

The preparation of Casp3 and cocrystals with covalently bound inhibitors followed protocols recently described.[15] Diffraction data were collected at IMCA-CAT beamline 17-ID at the advanced photon source (APS); Argonne. Diffraction data processing was completed as previously described.[15] The Casp3 structure bound with AcVDVAD-CHO (PDBid: 2h65) served as the search model. Model building and refinement were conducted iteratively using Phenix and Coot. Summary data collection and refinement statistics for both structures are given in Supporting Information: Table S1.

4.5 | Data analysis

GraphPad Prism version 9 (GraphPad Software) was used to calculate the IC_{50} by fitting the dose–response data with four-parameter variable slope nonlinear regression. These were transformed into pK_i values using the Cheng–Prusoff equation.[44] Since our compounds are covalent reversible inhibitors, they were characterized using pK_i values and not "k_{inact}/K_i", as would be necessary for covalent irreversible inhibitors.

ACCESSION CODES

Atomic coordinates of crystallographic complexes with Casp3 have been deposited with the RCSB protein Data bank with accession code 7uso (AcITVKD-CHO), 7usq (AcDVPD-CHO), 7usp (AcITV(Orn)D-CHO), 7rna (AcITV(Dab)D-CHO), and 7rng (AcITAKD-CHO).

ACKNOWLEDGMENTS

We thank Vivien Czipper for excellent technical assistance and Prof. Dr. Sigurd Elz for providing infrastructure. We thank Prof. Dr. Michelle Arkin for Casp2 and Casp3 plasmids and scientific discussion. Steffen Pockes was supported by the Deutsche Forschungsgemeinschaft (DFG, German Research Foundation, Forschungsstipendium 436921318) and the Fonds der Chemischen Industrie (SK-208/16). This study used resources of the Advanced Photon Source, a US Department of Energy (DOE) Office of Science User Facility operated for the DOE Office of Science by Argonne National Laboratory under Contract No. DE-AC02-06CH11357. Use of the IMCA-CAT beamline 17-ID (or 17-BM) at the Advanced Photon Source was supported by the companies of the Industrial Macromolecular Crystallography Association through a contract with Hauptman-Woodward Medical Research Institute. This study was supported from NIH grant R01-AG62199, Caspase-2 Probe Compounds (awarded to Karen H. Ashe and Michael A. Walters). The authors thank the Lucas Brothers Foundation for financial support. Open Access funding enabled and organized by Projekt DEAL.

CONFLICTS OF INTEREST

The authors declare no conflicts of interest.

ORCID

Steffen Pockes http://orcid.org/0000-0002-2211-9868

REFERENCES

[1] X. Zhao, L. A. Kotilinek, B. Smith, C. Hlynialuk, K. Zahs, M. Ramsden, J. Cleary, K. H. Ashe, *Nat. Med.* **2016**, *22*, 1268.
[2] J. B. Carroll, A. L. Southwell, R. K. Graham, J. P. Lerch, D. E. Ehrnhoefer, L.-P. Cao, W.-N. Zhang, Y. Deng, N. Bissada, R. M. Henkelman, *Mol. Neurodegener.* **2011**, *6*, 1.
[3] J. Pozueta, R. Lefort, E. M. Ribe, C. M. Troy, O. Arancio, M. Shelanski, *Nat. Commun.* **2013**, *4*, 1.
[4] P. Liu, B. R. Smith, M. L. Montonye, L. J. Kemper, K. Leinonen-Wright, K. M. Nelson, L. Higgins, C. R. Guerrero, T. W. Markowski, X. Zhao, *Sci. Rep.* **2020**, *10*, 1.
[5] B. R. Smith, K. M. Nelson, L. J. Kemper, K. Leinonen-Wright, A. Petersen, C. D. Keene, K. H. Ashe, *Acta Neuropathol. Commun.* **2019**, *7*, 1.
[6] P. Liu, B. R. Smith, E. S. Huang, A. Mahesh, J. P. G. Vonsattel, A. J. Petersen, R. Gomez-Pastor, K. H. Ashe, *Acta Neuropathol. Commun.* **2019**, *7*, 1.
[7] B. R. Hoover, M. N. Reed, J. Su, R. D. Penrod, L. A. Kotilinek, M. K. Grant, R. Pitstick, G. A. Carlson, L. M. Lanier, L.-L. Yuan, K. H. Ashe, D. Liao, *Neuron* **2010**, *68*, 1067.
[8] C. M. Troy, M. L. Shelanski, *Nat. Med.* **2016**, *22*, 1207.
[9] M. A. Miles, T. Kitevska-Ilioski, C. J. Hawkins, *Int. Rev. Cell. Mol. Biol.* **2017**, *332*, 155.
[10] M. Kurokawa, S. Kornbluth, *Cell* **2009**, *138*, 838.
[11] P. Fuentes-Prior, G. S. Salvesen, *Biochem. J.* **2004**, *384*, 201.
[12] A. Schweizer, C. Briand, M. G. Grütter, *J. Biol. Chem.* **2003**, *278*, 42441.
[13] R. V. Talanian, C. Quinlan, S. Trautz, M. C. Hackett, J. A. Mankovich, D. Banach, T. Ghayur, K. D. Brady, W. W. Wong, *J. Biol. Chem.* **1997**, *272*, 9677.
[14] N. A. Thornberry, T. A. Rano, E. P. Peterson, D. M. Rasper, T. Timkey, M. Garcia-Calvo, V. M. Houtzager, P. A. Nordstrom, S. Roy, J. P. Vaillancourt, *J. Biol. Chem.* **1997**, *272*, 17907.
[15] M. Bresinsky, J. M. Strasser, B. Vallaster, P. Liu, W. M. McCue, J. Fuller, A. Hubmann, G. Singh, K. M. Nelson, M. E. Cuellar, C. M. Wilmot, B. C. Finzel, K. H. Ashe, M. A. Walters, S. Pockes, *ACS Pharmacol. Transl. Sci.* **2022**, *5*, 20.
[16] T. Kitevska, D. M. Spencer, C. J. Hawkins, *Apoptosis* **2009**, *14*, 829.
[17] M. Mancini, C. E. Machamer, S. Roy, D. W. Nicholson, N. A. Thornberry, L. A. Casciola-Rosen, A. Rosen, *J. Cell Biol.* **2000**, *149*, 603.
[18] O. Julien, M. Zhuang, A. P. Wiita, A. J. O'Donoghue, G. M. Knudsen, C. S. Craik, J. A. Wells, *Proc. Natl. Acad. Sci. USA.* **2016**, *113*, E2001.
[19] T. G. Oliver, E. Meylan, G. P. Chang, W. Xue, J. R. Burke, T. J. Humpton, D. Hubbard, A. Bhutkar, T. Jacks, *Mol. Cell* **2011**, *43*, 57.
[20] A. M. Murphy, R. Dagnino, Jr., P. L. Vallar, A. J. Trippe, S. L. Sherman, R. H. Lumpkin, S. Y. Tamura, T. R. Webb, *J. Am. Chem. Soc.* **1992**, *114*, 3156.
[21] C. K. Marlowe, R. M. Scarborough, A. M. Laibelman, U. Sinha, B.-Y. Zhu. *US006046169A*, **2000**.
[22] C. Black, E. L. Grimm, E. Isabel, J. Renaud. *WO01/27085A1*, **2001**.
[23] C. A. Lipinski, F. Lombardo, B. W. Dominy, P. J. Feeney, *Adv. Drug Deliv. Rev.* **1997**, *23*, 3.
[24] M. Poreba, W. Rut, K. Groborz, S. J. Snipas, G. S. Salvesen, M. Drag, *Cell Death Differ.* **2019**, *26*, 2695.
[25] L.-Y. Sun, C. Chen, J. Su, J.-Q. Li, Z. Jiang, H. Gao, J.-Z. Chigan, H.-H. Ding, L. Zhai, K.-W. Yang, *Bioorganic Chem.* **2021**, *112*, 104889.
[26] H. M. Kumalo, S. Bhakat, M. E., Soliman, *Molecules* **2015**, *20*, 1984.
[27] J. Schröder, A. Klinger, F. Oellien, R. J. Marhöfer, M. Duszenko, P. M. Selzer, *J. Med. Chem.* **2013**, *56*, 1478.
[28] A. Carlesso, C. Chintha, A. M. Gorman, A. Samali, L. A. Eriksson, *Sci. Rep.* **2019**, *9*, 1.
[29] S. R. Chowdhury, S. Kennedy, K. Zhu, R. Mishra, P. Chuong, A. Nguyen, S. G. Kathman, A. V. Statsyuk, *Bioorg. Med. Chem. Lett.* **2019**, *29*, 36.
[30] N. London, R. M. Miller, S. Krishnan, K. Uchida, J. J. Irwin, O. Eidam, L. Gibold, P. Cimermančič, R. Bonnet, B. K. Shoichet, *Nat. Chem. Biol.* **2014**, *10*, 1066.
[31] D. Toledo Warshaviak, G. Golan, K. W. Borrelli, K. Zhu, O. Kalid, *J. Chem. Inf. Model.* **2014**, *54*, 1941.
[32] K. Zhu, K. W. Borrelli, J. R. Greenwood, T. Day, R. Abel, R. S. Farid, E. Harder, *J. Chem. Inf. Model.* **2014**, *54*, 1932.
[33] S. Xue, H. Liu, Z. Zheng, *J. Mol. Sci.* **2019**, *20*, 4850.
[34] B. Fang, G. Fu, J. Agniswamy, R. W. Harrison, I. T. Weber, *Apoptosis* **2009**, *14*, 741.
[35] J. Agniswamy, B. Fang, I. T. Weber, *FEBS J.* **2007**, *274*, 4752.
[36] J. Agniswamy, B. Fang, I. T. Weber, *Apoptosis* **2009**, *14*, 1135.
[37] J. B. Baell, G. A. Holloway, *J. Med. Chem.* **2010**, *53*, 2719.
[38] C. Aldrich, C. Bertozzi, G. I. Georg, L. Kiessling, C. Lindsley, D. Liotta, K. M. Merz, A. Schepartz, S. Wang, *ACS Cent. Sci.* **2017**, *3*, 143.
[39] K. Roos, C. Wu, W. Damm, M. Reboul, J. M. Stevenson, C. Lu, M. K. Dahlgren, S. Mondal, W. Chen, L. Wang, *J. Chem. Theory Comput.* **2019**, *15*, 1863.
[40] M. C. Maillard, F. A. Brookfield, S. M. Courtney, F. M. Eustache, M. J. Gemkow, R. K. Handel, L. C. Johnson, P. D. Johnson, M. A. Kerry, F. Krieger, M. Meniconi, I. Muñoz-Sanjuán, J. J. Palfrey, H. Park, S. Schaertl, M. G. Taylor, D. Weddell, C. Dominguez, *Bioorg. Med. Chem.* **2011**, *19*, 5833.
[41] D. Chauvier, S. Renolleau, S. Holifanjaniaina, S. Ankri, M. Bezault, L. Schwendimann, C. Rousset, R. Casimir, J. Hoebeke, M. Smirnova, G. Debret, A.-P. Trichet, Y. Carlsson, X. Wang, E. Bernard, M. Hébert, J.-M. Rauzier, S. Matecki, A. Lacampagne, P. Rustin, J. Mariani, H. Hagberg, P. Gressens, C. Charriaut-Marlangue, E. Jacotot, *Cell Death Dis.* **2011**, *2*, e203.
[42] I. C. Choong, W. Lew, D. Lee, P. Pham, M. T. Burdett, J. W. Lam, C. Wiesmann, T. N. Luong, B. Fahr, W. L. DeLano, R. S. McDowell, D. A. Allen, D. A. Erlanson, E. M. Gordon, T. O'Brien, *J. Med. Chem.* **2002**, *45*, 5005.

[43] M. B. Boxer, A. M. Quinn, M. Shen, A. Jadhav, W. Leister, A. Simeonov, D. S. Auld, C. J. Thomas, *ChemMedChem* **2010**, *5*, 730.
[44] Y.-C. Cheng, W. H. Prusoff, *Biochem. Pharmacol.* **1973**, *22*, 3099.

SUPPORTING INFORMATION

Additional supporting information can be found online in the Supporting Information section at the end of this article.

How to cite this article: M. Bresinsky, J. M. Strasser, A. Hubmann, B. Vallaster, W. M. McCue, J. Fuller, G. Singh, K. M. Nelson, M. E. Cuellar, B. C. Finzel, K. H. Ashe, M. A. Walters, S. Pockes, *Arch. Pharm*. **2022**;355:e2200095.
https://doi.org/10.1002/ardp.202200095